CAPITAL UNIVERSITY OF SCIENCE AND TECHNOLOGY, ISLAMABAD

Formation and Trajectory Tracking of Multiple UAVs using Adaptive and Robust Control Methods under Disturbances

by

Muhammad Amir Khan

A thesis submitted in partial fulfillment for the degree of Master of Science

in the

Faculty of Engineering
Department of Electrical Engineering

2022

Dedicated to my exceptional parents, adored siblings, and professors whose tremendous support and cooperation led me to this wonderful accomplishment.

CERTIFICATE OF APPROVAL

Formation and Trajectory Tracking of Multiple UAVs using Adaptive and Robust Control Methods under Disturbances

by

Muhammad Amir Khan

(MEE193008)

THESIS EXAMINING COMMITTEE

S. No.	Examiner	Name	Organization
(a)	External Examiner	Dr. Qudrat Khan	COMSATS, Islamabad
(b)	Internal Examiner	Dr. Aamer Iqbal Bhatti	CUST, Islamabad
(c)	Supervisor	Dr. Fazal Ur Rehman	CUST, Islamabad

Dr. Fazal Ur Rehman
Thesis Supervisor
January, 2023

Dr. Noor Muhammad Khan
Head
Dept. of Electrical Engineering
January, 2023

Dr. Imtiaz Ahmad Taj
Dean
Faculty of Engineering
January, 2023

Author's Declaration

I, **Muhammad Amir Khan** hereby state that my MS thesis titled "**Formation and Trajectory Tracking of Multiple UAVs using Adaptive and Robust Control Methods under Disturbances**" is my own work and has not been submitted previously by me for taking any degree from Capital University of Science and Technology, Islamabad or anywhere else in the country/abroad.

At any time if my statement is found to be incorrect even after my graduation, the University has the right to withdraw my MS Degree.

Muhammad Amir Khan
Registration No: MEE193008

Plagiarism Undertaking

I solemnly declare that research work presented in this thesis titled "**Formation and Trajectory Tracking of Multiple UAVs using Adaptive and Robust Control Methods under Disturbances**" is solely my research work with no significant contribution from any other person. Small contribution/help wherever taken has been duly acknowledged and that complete thesis has been written by me.

I understand the zero tolerance policy of the HEC and Capital University of Science and Technology towards plagiarism. Therefore, I as an author of the above titled thesis declare that no portion of my thesis has been plagiarized and any material used as reference is properly referred/cited.

I undertake that if I am found guilty of any formal plagiarism in the above titled thesis even after award of MS Degree, the University reserves the right to withdraw/revoke my MS degree and that HEC and the University have the right to publish my name on the HEC/University website on which names of students are placed who submitted plagiarized work.

Muhammad Amir Khan
Registration No:MEE193008

Acknowledgement

I am thankful to my Creator Allah Subhana-Watala to have guided me throughout this work at every step and for every new thought which You set up in my mind to improve it. Indeed, I could have done nothing without Your priceless help and guidance. Whosoever helped me throughout the course of my thesis, whether my parents or any other individual was Your will, so indeed none be worthy of praise but You. I am profusely thankful to my beloved parents who raised me when I was not capable of walking and continued to support me throughout every department of my life.

I would also like to express special thanks to my supervisor Dr. Fazal Ur Rehman for his help throughout my thesis and also for the courses that he has taught me.

I would also like to express special thanks to my head of the electrical department Dr. Noor Muhammad Khan for his tremendous support and cooperation throughout my thesis.

I would also like to express special thanks to Dr. Nasim Ullah for his tremendous support and cooperation. Each time I got stuck in something, he came up with a solution. Without his help, I wouldn't have been able to complete my thesis. I appreciate his patience and guidance throughout the whole thesis.

Finally, I would like to express my gratitude to all the individuals who have rendered valuable assistance to my study.

Muhammad Amir Khan

Abstract

Multiple Unmanned Aerial Vehicles (UAVs) have numerous applications in various areas such as surveillance, industrial automation, and disaster management equipped with Leader follower configurations. Advance and robust control strategies make sure the safety, reliability, and accuracy of the crucial task performed by the Multiple UAVs. Multiple UAVs are governed by two separate controllers, namely formation and trajectory tracking controllers respectively. A challenging task was to design the controller under environmental effects, disturbances due to wind, and parametric uncertainties. This thesis proposes a robust adaptive formation and trajectory tracking control of Multiple UAVs using a simple backstepping controller, integral backstepping controller, and Super twisting sliding mode controller (STSMC), also showing the comparison between them. All controllers are tested using numerical simulations performed in MATLAB/Simulink. From the results presented, it is verified that the integral backstepping controller shows no chattering phenomena and shows minimum error in tracking the desired reference trajectories in all dynamics of the UAV under wind disturbance.

keywords: Unmanned Aerial Vehicles, adaptive robust control, super twisting sliding mode control, integral backstepping Control, trajectory control, formation control

Contents

List of Figures

List of Tables

Abbreviations

ASTSMC	Adaptive Super Twisting Sliding Mode Control
LMI	Linear Matrix Inequalities
PID	Proportional-Integral-Derivative
SMC	Sliding Mode Control
STSMC	Super Twisting Sliding Mode Control
UAV	Unmanned Aerial Vehicle

Symbols

θ_i	Pitch angle of i^{th} quad-copter [rad]
ϕ_i	Roll angle of i^{th} quad-copter [rad]
ψ_i	Yaw angle of i^{th} quad-copter [rad]
X_i, Y_i, Z_o	X,Y,Z Position of i^{th} quad-copter in earth coordinates [m]
$\dot{X}_i, \dot{Y}_i, \dot{Z}_i$	Velocity of i^{th} quad-copter in earth coordinates [m/sec]
$\ddot{X}_i, \ddot{Y}_i, \ddot{Z}_i$	Acceleration of i^{th} quad-copter in earth coordinates [m/sec^2]
Ω_{ri}	Overall speed of the propellers of i^{th} quad-copter [rad/sec]
J_{ri}	Rotor inertia of i^{th} quad-copter [kg.m^2]
g	Acceleration due to gravity [m/sec^2]
D_{Xi}, D_{Yi}	Uncertainty in $\ddot{X}, \ddot{Y}$ dynamics of i^{th} quad-copter [m/sec^2]
I_{xi}, I_{yi}, I_{zi}	moments of i^{th} quad-copter inertia in X, Y and Z coordinates [kg.m^2]
m_{Qi}	mass of i^{th} quad-copter [kg]

Chapter 1

Introduction

1.1 Introduction

This research work proposes a robust adaptive formation and trajectory tracking control of Multiple UAVs using a simple backstepping controller, integral backstepping controller, and Super twisting sliding mode controller (STSMC), also showing the comparison between them.

The research done for this thesis has been presented in six sections. The first section relates to the introduction, background history, and summary. The second section relates to literature review, gap analysis, and problem statement. The literature review entails locating, assessing, and synthesising relevant literature on the topic. A gap analysis is the process of determining the difference between the existing and intended level of knowledge. A gap analysis in the context of a literature review entails identifying research projects that have not yet been done or areas where there is a lack of knowledge. The third section relates to system mathematical modeling and description. Modeling of a single quad-copter and transnational dynamics of multiple UAVs are the main objective of this section. The fourth section includes the formation controller and trajectory controller formulations. The fifth section relates to the comparative analysis and simulation

FIGURE 1.1: History of drones balloons [40]

results for proposed different controllers. At the end, conclusions and future work are mentioned.

1.1.1 Background

The concept of drones takes us back to 1849 when Austria attacked Venice using an automated air balloon filled with explosives [40]. While the Austrian army surrounded Venice, two hundred rounds of explosives were fired over the city. With each ball weighing between twenty to thirty pounds, it caused a widespread destruction with each impact on the city. Luckily for the Venetians, only one was on the spot while the others were winded away as the strong wind currents changed their course of impact.Although this military technology effort is groundbreaking, the use of hot air balloons doesn't really fit the profile of being called "drones" let alone, military drones, but it's interesting to see how the military cavalry thought of the basic concept of a drone more than 170 years ago, this mindset will drive the evolution of drone technology for centuries and decades to come.

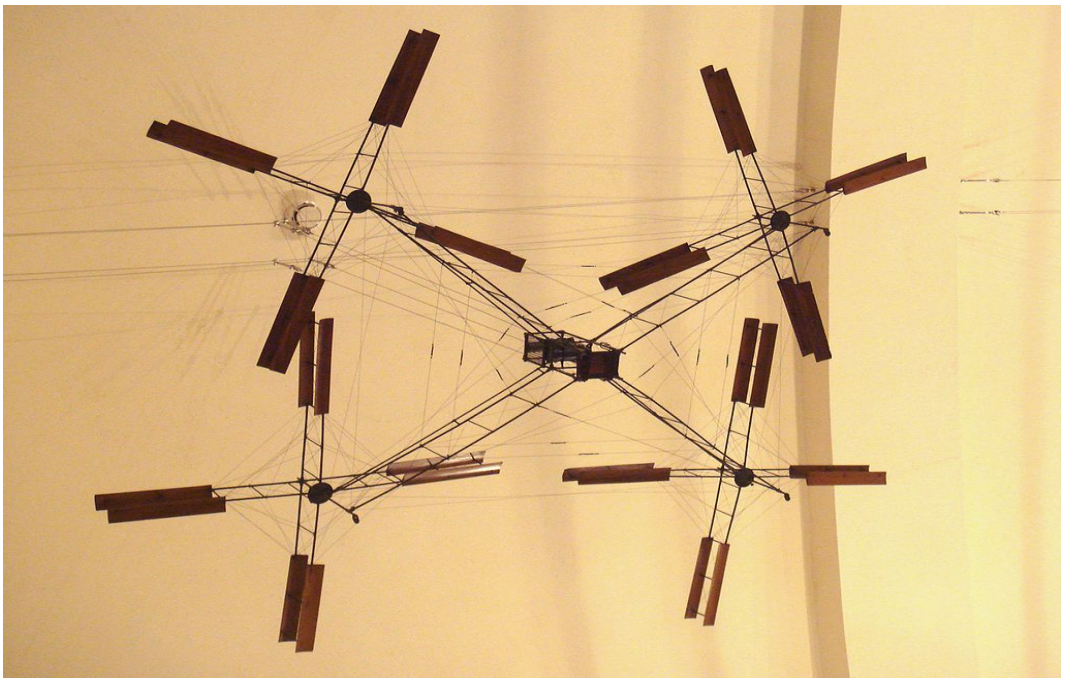

FIGURE 1.2: Initial design of drone quad [40]

The most common feature that can be seen in modern - commercial drone designs is their quad-copter configuration. It was the Breguet brother - Jacques and Louis who came up with the early development technology of commercial drones in 1907. With the help of French Physiologist - Professor Charles Richet, the Breguet brothers were able to develop an early example of the helicopter's predecessor, the autogyro. [40].

The design of Copter at the time was progressive. He made the first-ever vertical lift of an aircraft. Sadly, it elevated only 0.6 meters high. There a total of four people were needed for the stability of the structure so it was not considered a free-flying structure. However, it has been shown that the quad-copter concept is suitable for flying. More technical development will be needed to make it viable.

Commercial drones have been a very hot topic in the past decade. With increasing interest in drones, more innovative and interactive have been playing their part in the development of these drones. Prior to 2010 drones were specifically used for military or personal purposes. Although with the new decades, new commercial applications of drones have been proposed, including the use use of drone systems

FIGURE 1.3: Modern day Quad-copter [40]

in vehicles. Seeing the popularity of drones being increased, The FAA issued a license for the production of over 1000 drones by 2015 due to high market demand.

The market demand has grown three times since then and is growing exponentially since then. Drones have made their way into the market by being infused with every everyday use gadget. From photo-shoot cameras to aircraft and smartphones, everything is embedded with drone technology.

1.1.2 Summary

Throughout history, swarming has been a military tactic. People of Scythians, Bronze age, and even the Mongols and Turks of the early middle ages in groups adopted variations of tactics. The armies of the steppe peoples consisted mainly of lightly armed mounted archers. They were particularly effective against the formations of the Western armies dominated by rigid infantry [41]. Rapid growth in technology has led to the use of fixed-winged aircraft into a hobby. From micro-controllers and accelerometers to camera sensors all have adapted to a single technology. On top of that, recent achievements and development in drone

technology, it has now made it possible to fly drones with four or more rotors by simply adjusting the speed of every individual rotor.

These advancements in drone technology open up newer possibilities for multi-rotor aircraft. Due to these achievements, these drones can be given more speed, and stability and enhance their performance which makes them viable for use in defense, aerial photography, search and rescue programs, oil subject monitoring, agriculture, and suspended freight delivery. [1].

Some war theorists advocate swarming tactics as the next step in the evolution of the military doctrine, a "game-changer" that uses industry terminology. Building a simple battlefield robot using an algorithm can mimic a swarm of bees or ants with a great strategic advantage. Elements of swarm tactics have been used by the military for thousands of years, but corps of automated vehicles could improve these maneuvers and add a new dimension to warfare [41].

Chapter 2

Literature Review

2.1 Introduction

Formation flight consists of multiple UAVs maintaining the relative distance among them during operation. In recent times, a lot of attention has been diverted toward formation flights and their controllers. Because of the capability applications of drone technology in defensive enterprises, aerial photography, search and rescue operations, oil subject monitoring projects, and agricultural and suspended freight delivery. [1]. Multiple UAVs cover more area with multiple payloads as compared to single payload attached UAVs [2–6]. However, while facing uncertainties and disturbances during flight, it can be a very difficult challenge to control multiple UAV formations. The quad-copters six degrees of Freedom nonlinear differential equations are modified around the transnational and rotational dynamics [7–10].

Multiple formations can be achieved by formation controller, here in this thesis inverted V shape formation is maintained, in which the leader is at the Vertex of inverted V and two followers are at the tails of the inverted V. With the use of suitable control schemes, the modeling uncertainties and the disturbances due to gust can be compensated. This can be ensured with robust formation, to compensate for the uncertainties and disturbances introduced at any time.

2.2 Gap Analysis

To resolve the problems of the formation controller of the quadrotor, many research efforts have been made. In [11], for multiple UAVs generic PID controller with a sliding mode controller (SMC) is used. In [12] for the formation pattern, a proportional derivative and the fuzzy logic system are proposed by the leader-follower formation control. In [13–15], for formation control problems, the SMC method is proposed for multiple UAVs.Multiple UAVs circular trajectory control formation scheme is discussed in [16]. In [17], A prescribed controller, which ensures a robust formation pattern and trajectory is also designed to control the formation of multiple UAVs. In [18] The controller does not leave any room for errors or any delay in communication between multiple UAVs. Two UAVs trajectory controller based on PI controller is presented in [19]. Likewise, a nonlinear controller for multiple UAVs is discussed in [20]. With the use of a prior-bounded intermediary controller design, it gives the UAVs orientation and control trust [21].

Similar to the prior-bounded intermediary controller, a non-linear controller also plays a very similar role for multiple UAVs using the gain-turning method [22, 23]. Using a tracking controller for the formation control with an attached payload based on the Lyapunov function [24]. To address the formation and tracking control of the quad-copters, a formation controller was designed which overcame these problems by avoiding collision between multiple UAVs swarm [25]. An adaptive control algorithm is presented in [26]. External disturbances and motion constraints for the swarm formation are discussed in [27]. ASTSMC and STSMC controllers are used in leader-follower UAVs configuration with parametric uncertainties and disturbances [38].

All of the work cited above directly reflects on different designs and methods used for the formation of multiple UAVs. The background of the robust and non-linear control system, itself shows its importance in the control system community today. For uncertain systems, the robust control is designed with a bounded set [28]. Both time and frequency domains are kept in the equation to design robust controllers.

H_∞ controller is designed in the frequency domain introduced in [28]. Later with the use of Riccati equations [30], loop shaping [29], and Linear Matrix Inequalities (LMIs) [31], H_∞ many variations were reported. The control system performance varies on certain parameters like loop gains, phase margins, settling time, rise time, delay time, and overshoot percentage in the excitation signals. The state space framework reveals the modern approach to designing a robust controller. The Sliding Mode Controller has made its way into numerous applications in science and technology, becoming the most widely used controller [32]. SMC variants such as LMI based SMC [33], global sliding mode [34], higher-order SMC [35, 36], and non-singular terminal SMC [37]. In [38] author proposed STSMC and ASTSMC controllers for leader-follower configuration under uncertainties and disturbances.

The summary of the limitations of previous research are also shown at Table 2.1.

TABLE 2.1: Gap Analysis

Reference	**Authors, Year**	**Proposed Controller**	**Limitations**
[11]	Wua, F.; Chen, J.; Liang, Y, 2017	Classical PID control scheme with a sliding mode controller (SMC)	A Classical PID control scheme is used for multiple quadrotors with a sliding mode controller (SMC). However, the PID-SMC mentioned above does not take disturbances and communication delays between multiple UAVs into consideration.

[12]	Abbas, R., Wu, Q, 2015	Fuzzy Logic controller	The author suggested the use of leader-follower formation controller using the simple proportionality derivative controller paired with the fuzzy logic system. Unfortunately, the above controller did not consider any uncertainties in the equation.
[13]	Khaled, A.G.; Youmin, Z, 2015	Classical SMC	A traditional SMC method was taken into consideration. However, what makes this formation at fault is that the SMC method offers high-frequency chattering in the extinction signal which in response, degrades the life of actuators.
[26]	Estevez, J.; Grana, M., 2017	Adaptive control algorithm	A model reference adaptive control algorithm is presented for a swarm three quadrotors. The gains of the controller are turned online. With this, the algorithm of the system is able to adapt to unexpected disturbances. However, no robust investigation is carried out in this method.

[27]	Liang, Y.; Dong, Q.; Zhao, Y., 2020	Adaptive Leader Follower Formation Control	Adaptive control laws for the formation of swarm UAVs subject to movement restrictions and unknown external perturbations are discussed.
[38]	Mehmood, Y.; Aslam, J.;Ullah, N.; Chowdhury, M.SK.; Alzaed, A.N., 2021	STSMC and ASTSMC Controllers	The authors proposed robust trajectory tracking with parametric uncertainties and disturbances for quad and swam formation, however, in the excitation signals high-frequency chattering is observed in SMC methods as the life of the actuators is drastically reduced by chattering phenomena.

2.3 Problem Statement

The previously implemented method performed well based on the proposed design but had some limitations or drawbacks as discussed in the literature review. Some of the proposed controllers are highly complex models, do not consider uncertainties, have time delays, have high-frequency chattering in the excitation signal, are proposed only for attitude and position controllers, and are proposed only for formation controllers.

Keeping all of these limitations into consideration my contribution would be proposing an integral backstepping controller for the multiple UAVs flying the leader-follower configuration under wind disturbances.

2.4 Summary

A literature review is an essential part of any research endeavour since it helps to obtain a thorough overview of the current information in field of study. The literature review entails locating, assessing, and synthesising relevant literature on the topic. A gap analysis is the process of determining the difference between the existing and intended level of knowledge. A gap analysis in the context of a literature review entails identifying research projects that have not yet been done or areas where there is a lack of knowledge. This can aid in identifying research areas that are most likely to make a substantial contribution to the field of study. A problem statement is a clear and concise statement of the research problem or objective that are trying to address. It clearly identify the research question, the significance of the problem, and the scope of the research. This chapter thoroughly covers all the above mentioned literature review, gap analysis, and problem statement done for the process of this thesis.

Chapter 3

System Description and Mathematical Modeling

Mathematical modeling transforms problems in the application domain into manageable mathematical formulas by use of hypotheses and arithmetic analysis providing insights and useful recommendations for building applications. Mathematical modeling is useful in a variety of applications, providing precise strategies for problem solving and systematic understanding of the modeled system. It also enables better system design, control and efficient use of modern computing capabilities.

3.1 Quad-copter Dynamic Model

Fig. 3.1 represents a UAV quad-copter with Earth coordinates $R_E\,(O, X, Y, Z)$. UAV body coordinates are specified as $R_B\,(O_B, X_B, Y_B, Z_B)$ without considering the inertial coordinate system. let denote by m the mass of the UAV, g represent the gravity acceleration, and from center of gravity to center of each rotor is denoted by l. Whereas, ϕ, θ, and ψ represents the euler pitch, roll and yaw angles.

The following assumptions were made to construct the model.

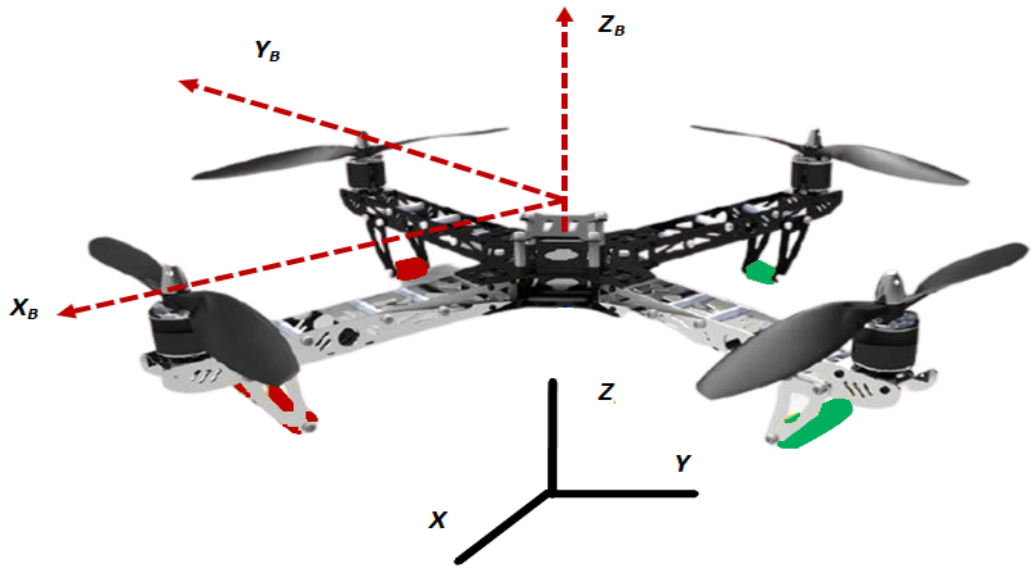

FIGURE 3.1: Quad-copter in inertial reference frame

Assumption 1: The UAV is assumed to be represented by a symmetric rigid body configuration with mass m.

Assumption 2: The External acceleration disturbance will only affect each UAV's X and Y dynamics.

Assumption 3: External disturbances affect each UAV uniformly.

Based on the assumptions mentioned above, in the quad-copter UAV each motor produces force $F_i (i = 1, 2, 3, \text{ and } 4)$ is proportional to the square of the angular speed. As F_i is always positive then the quad-copter UAV motors will only turn in only one direction.

The front right and rear left motors (M1 and M3) rotate in a counter-clockwise direction, as the front left and rear right motors (M2 and M4) rotate in a clockwise direction. In a properly trimmed flight, the Aerodynamic torques and gyroscopic effects tend to cancel each other.

As F represents the total thrust which is the sum of the individual trusts of each motor.

The quad-copter orientation is denoted by the rotational matrix $R : R_E \rightarrow R_B$ depending upon the Euler angles resulting in the following equation:

$$R(\phi,\theta,\psi) = \begin{bmatrix} \cos\psi\cos\theta & \sin\phi\sin\theta\cos\psi - \sin\psi\cos\theta & \cos\phi\cos\theta\cos\psi + \sin\psi\sin\phi \\ \sin\psi\cos\theta & \sin\phi\sin\theta\sin\psi + \cos\psi\cos\theta & \cos\phi\cos\theta\sin\psi - \sin\phi\cos\psi \\ -\sin\theta & \sin\phi\cos\theta & \cos\phi\cos\theta \end{bmatrix} \tag{3.1}$$

The drag on the propellers and body of the quad-copter UAV and the thrust of the rotors generate the external torques. Gyroscopic effects of motors also generate moments that are to be considered. The ith rotor of quad-copter UAV thrust force is formulated to be:

$$F_i = \frac{1}{2}\rho\Lambda C_T r^2 {\omega_i}^2 = b{\omega_i}^2, \tag{3.2}$$

where r and Λ represent the radius and section of the propeller, ρ represents the air density, and C_T represents the aerodynamic thrust coefficient.

The drag force at the propeller of the ith rotor and opposed motor torque cause the aerodynamic drag torque which is defined as:

$$\delta_i = \frac{1}{2}\rho\Lambda C_D r^2 {\omega_i}^2 = d{\omega_i}^2 \tag{3.3}$$

The C_D represents the aerodynamic drag coefficient. The two constants $d > 0$ and $b > 0$ depend upon the air density, as the drag, lift coefficient and the geometry of the propellers are shown in Eq. 3.2 and 3.3. The pitching torque is a function of the difference $(F_3 - F_1)$, similarly, rolling and yawing torques are formulated as follows:

$$\tau_\theta = l(F_3 - F_1) \tag{3.4}$$

$$\tau_\phi = l(F_4 - F_2) \tag{3.5}$$

$$\tau_\psi = C(F_1 - F_2 + F_3 - F_4) \tag{3.6}$$

where C is the proportional coefficient. Due to the motion of the quad-copter UAV body and the propellers, two gyroscopic resultant torques are produced, defined below:

$$M_{gp} = \sum_{i=1}^{4} \Omega\Lambda \begin{bmatrix} 0 & 0 & J_r(-1)^{i+1}\omega_i \end{bmatrix}^T \tag{3.7}$$

$$M_{gp} = \Omega\Lambda J\Lambda, \tag{3.8}$$

where Ω represents the angular velocity vector in the earth's fixed frame, the control inputs formulated for the varying speed of the four rotors of the quad-copter UAV, are shown as:

$$u = \begin{bmatrix} u_1 \\ u_2 \\ u_3 \\ u_4 \end{bmatrix} = \begin{bmatrix} F \\ \tau_\phi \\ \tau_\theta \\ \tau_\psi \end{bmatrix} = \begin{bmatrix} b & b & b & b \\ 0 & -lb & 0 & lb \\ -lb & 0 & lb & 0 \\ d & -d & d & -d \end{bmatrix} \begin{bmatrix} {\omega_1}^2 \\ {\omega_2}^2 \\ {\omega_3}^2 \\ {\omega_4}^2 \end{bmatrix} \tag{3.9}$$

From Eq. 3.9, the input u_1 denotes the total thrust force on the quad-copter UAV body in the z-axis, the inputs u_2, u_3 and u_4 denote the rolling, pitching and yawing torque, respectively.

Using the Newton-Euler formalism for dynamic modeling, the dynamic governing equations of quad-copter appears as:

$$\begin{cases} m\ddot{\zeta} = F_{th} + F_d + F_g \\ J\dot{\Omega} = M - M_{gp} - M_{gb} - M_a, \end{cases} \tag{3.10}$$

Where $F_{th} = R(\phi, \theta, \psi)\left[0, 0, \sum_{i=1}^{4} F_i\right]^T$ represents the total thrust force of all rotors, $F_d = diag(k_1, k_2, k_3)\dot{\zeta}^T$ represents the air drag force, $F_g = [0, 0, mg]^T$ represents the gravitational force, $M = [\tau_\phi, \tau_\theta, \tau_\psi]^T$ represents the total rolling, pitching and yawing torques, respectively, $M_g b$ and $M_g p$ represents the gyroscopic torques and $M_a = diag(k_4, k_5, k_6)\left[\dot{\phi}^2, \dot{\theta}^2, \dot{\psi}^2\right]^T$ represents the aerodynamic frictional torque.

By putting the forces and position vector into Eq. 3.10 results in the transnational and rotational dynamics of the quad-copter UAV which are expressed below:

$$\ddot{X}_i = U_{1i}(\cos\psi_i \sin\theta_i \cos\phi_i + \sin\psi_i \sin\phi_i)\frac{1}{m_{Qi}} - D_{Xi}, \tag{3.11}$$

$$\ddot{Y}_i = U_{1i}(\sin\psi_i \sin\theta_i \cos\phi_i - \cos\psi_i \sin\phi_i)\frac{1}{m_{Qi}} - D_{Yi}, \tag{3.12}$$

$$\ddot{Z}_i = g - U_{1i}(\cos\theta_i \cos\phi_i)\frac{1}{m_{Qi}} - D_{Zi}, \tag{3.13}$$

$$\ddot{\phi}_i = \frac{I_{yi} - I_{zi}}{I_{xi}}\dot{\theta}_i\dot{\psi}_i + U_{2i}\frac{l_i}{I_{xi}} - \frac{J_{ri}}{I_{xi}}\dot{\theta}_i\Omega_{ri} - D_{\phi i}, \tag{3.14}$$

$$\ddot{\theta}_i = \frac{I_{zi} - I_{xi}}{I_{yi}}\dot{\phi}_i\dot{\psi}_i + U_{3i}\frac{l_i}{I_{yi}} - \frac{J_{ri}}{I_{yi}}\dot{\phi}_i\Omega_{ri} - D_{\theta i}, \tag{3.15}$$

and,

$$\ddot{\psi}_i = \frac{I_{xi} - I_{yi}}{I_{zi}}\dot{\phi}_i\dot{\theta}_i + U_{4i}\frac{l_i}{I_{zi}} - D_{\psi i} \tag{3.16}$$

Eq. 3.11-3.16 represent the overall mathematical model of the UAV quad-copter, where i is an indication for $[L, f]$, where $f = [F1, F2]$. The subscript L is an indication for the Leader UAV, while $F1$ and $F2$ indicates the follower 1 and 2, respectively.

Now are are ready to display the error dynamics for the formation control.

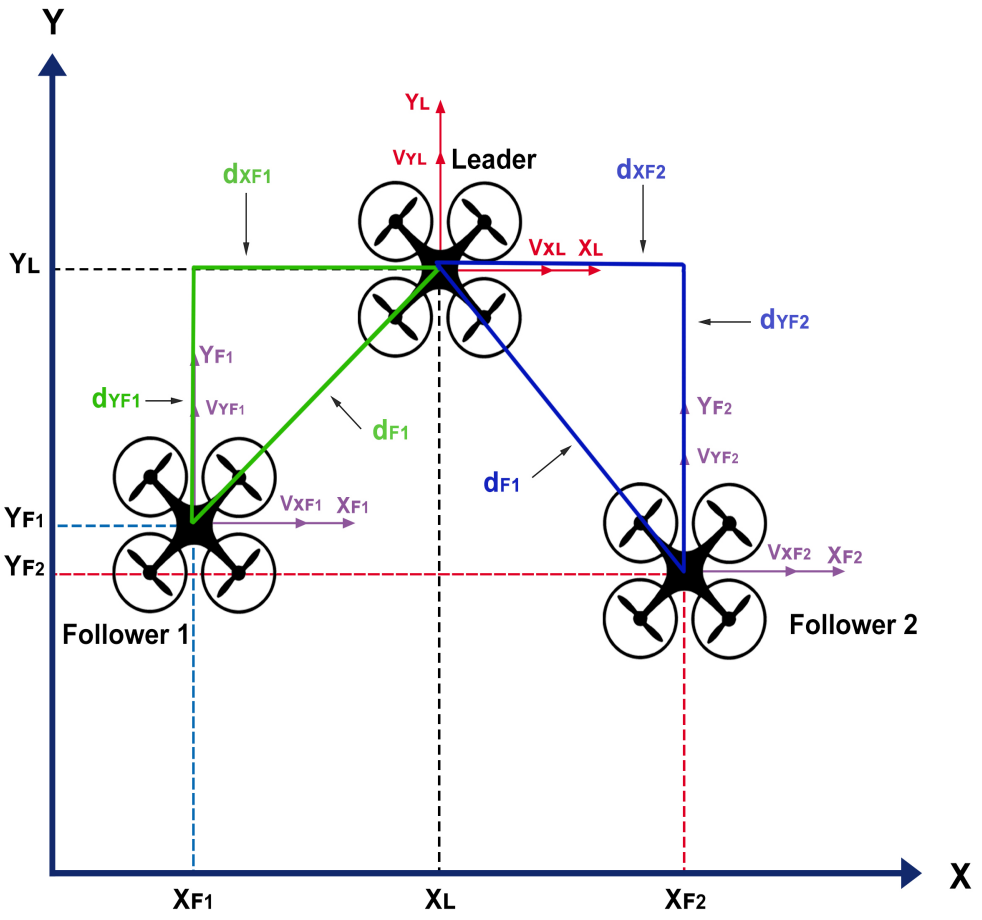

FIGURE 3.2: Leader-Follower configuration

3.2 Formation Error Dynamic Model

The overall dynamics model is shown in Eq. 3.11-3.16. Fig. 3.2 and 3.3 represents the leader-follower configuration of Multiple quad-copters. The transnational dynamics are defined as,

$$\dot{X}_i = V_{Xi}\cos(\psi_i) - V_{Yi}\sin(\psi_i) \tag{3.17}$$

and,

$$\dot{Y}_i = V_{Xi}\sin(\psi_i) + V_{Yi}\cos(\psi_i) \tag{3.18}$$

and the angular error dynamics are,

$$\dot{\psi_L} = \omega_L \tag{3.19}$$

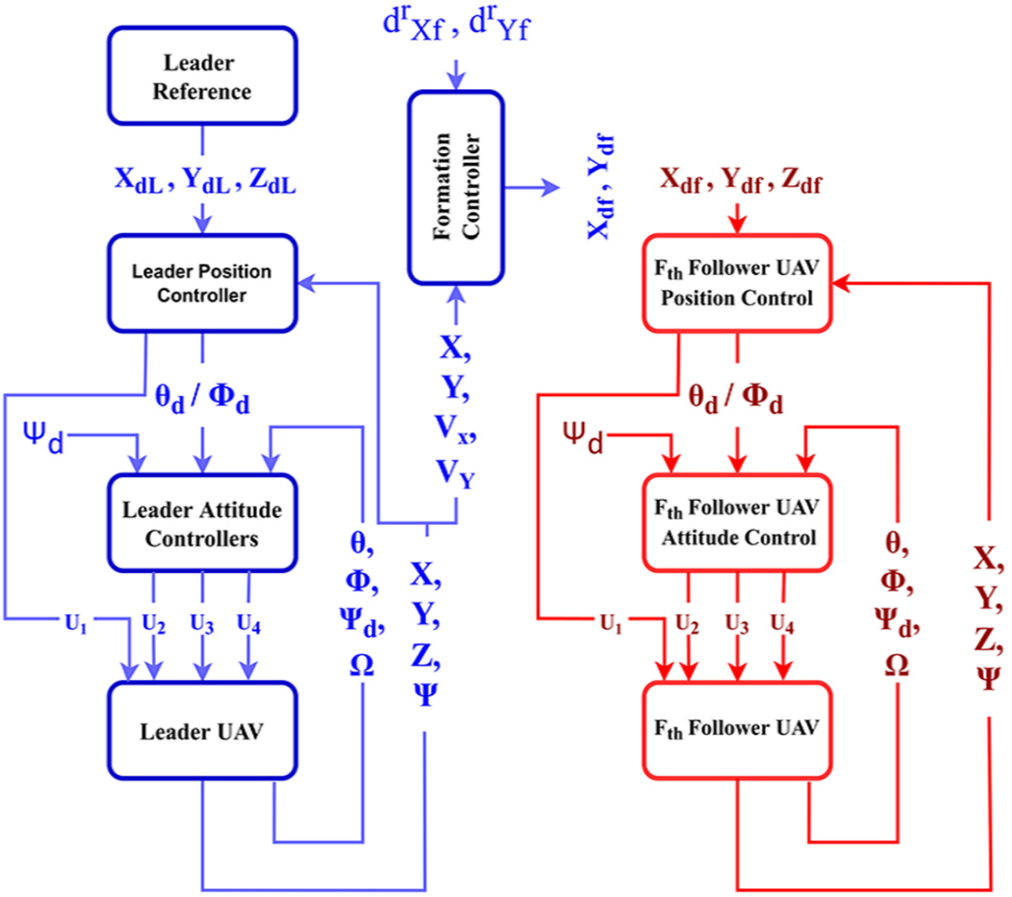

FIGURE 3.3: Block diagram

In inertial frame V_{Xi} and V_{Yi} represents X and Y directional velocities. Assuming the follower UAV maintains a distance of d_{Xf} and d_{Yf} in the X and Y planes, respectively, from the leading UAV. Mathematically, d_{Xf} and d_{Yf} are expressed as follows:

$$d_{Xf} = -\sin(\psi_L)(Y_L - Y_f) - \cos(\psi_L)(X_L - X_f) \tag{3.20}$$

and,

$$d_{Yf} = -\cos(\psi_L)(Y_L - Y_f) - \sin(\psi_L)(X_L - X_f) \tag{3.21}$$

where $d_{Xf} = d_i \cos(\phi)$, $d_{Yf} = d_i \sin(\phi)$ and $X_f = [X_{F1}, X_{F2}]$. On the other hand, the ψ error dynamics is defined as : $e_\psi = \psi_f - \psi_L$. Taking the 1st time derivative

of Eq. 3.20 and 3.21 and then computing along Eq. 3.17 and 3.18 results in the following equations:

$$\dot{d}_{Xf} = d_{Yf}\omega_L - V_{Yf}\sin(e_\psi) + V_{Xf}\cos(e_\psi) - V_{XL} \tag{3.22}$$

$$\dot{d}_{Yf} = -d_{Xf}\omega_L + V_{Yf}\cos(e_\psi) + V_{Xf}\sin(e_\psi) - V_{YL} \tag{3.23}$$

where V_{YL}, V_{Xf}, and V_{Yf} represents velocities in longitudinal and lateral regions of the leader UAV and its respective follower UAVs as follower 1, and follower 2. The error equation between regional dynamics of lateral and longitudinal Eq. 3.22 and 3.23 is shown below:

$$\dot{X} = F(X) + G(X)v \tag{3.24}$$

where, $X = \begin{bmatrix} e_{Xf} \\ e_{Yf} \\ e_\psi \end{bmatrix}, \dot{X} = \begin{bmatrix} \dot{e_{Xf}} \\ \dot{e_{Yf}} \\ \dot{e_\psi} \end{bmatrix}, v = \begin{bmatrix} V_{Xf} \\ V_{Yf} \\ \omega_F \end{bmatrix}$ are position, velocity, and control input vectors. In addition $F(X)$ and $G(X)$ are nonlinear vector fields which are explained as:

$$F(X) = \begin{bmatrix} e_{Yf}\omega_L + V_{XL} - \omega_L d^d_{Yf} \\ -e_{Xf}\omega_L + V_{YL} - \omega_L d^d_{Xf} \\ e_\psi \end{bmatrix} \tag{3.25}$$

$$G(X) = \begin{bmatrix} -\cos(e_\psi) & \sin(e_\psi) & 0 \\ -\sin(e_\psi) & -\cos(e_\psi) & 0 \\ 0 & 0 & 1 \end{bmatrix} \tag{3.26}$$

It is important to report that the reference trajectories for the followers' UAVSs are:

$$X_{df} = X_L - d_{Yf}\sin(\psi_L) - d_{Xf}\cos(\psi_L) \tag{3.27}$$

$$Y_{df} = Y_L - d_{Yf}\cos(\psi_L) - d_{Xf}\sin(\psi_L) \tag{3.28}$$

Now, the mismatch between the reference trajectories ad the actual trajectories of the quad-copters can be defined as $e_{Xf} = d^d_{Xf} - d_{Xf}$ and $e_{Yf} = d^d_{Yf} - d_{Yf}$. The detailed formation error dynamics are presented. Now it is suitable to summarize the chapter.

3.3 Summary

Quad-copters are indeed considered under-actuated systems, meaning that there are fewer control inputs than degrees of freedom. This can make them challenging to model and control, as there are not enough inputs to directly control all the states of the system. Modeling an under-actuated quad-copter requires a detailed understanding of the system's dynamics, including the effects of aerodynamics, propulsion, and actuator dynamics. The model should take into account the nonlinearities that arise from the system's under-actuation, such as the coupling between different states and the constraints on the control inputs. In addition, modeling an under-actuated quad-copter also requires taking into account the physical limitations and constraints of the system, such as the maximum rotor speed, the maximum torque and thrust produced by the rotors, and the maximum tilt angles of the aircraft. This chapter briefly explains the overall transnational and rotational dynamic modeling of the quad-copter under mentioned assumptions. Furthermore, the formation flight controller and its transnational dynamics have also been addressed to follow up the swarm formation in the inverted V style.

Chapter 4

Formation and Trajectory Controller Formation

In this section, first, all the formulations of formation and trajectory controllers are designed accordingly to ASTSMC, then second accordingly to the backstepping controller, and finally third accordingly to the Integral backstepping controller.

4.1 Adaptive Super Twisting Sliding Mode Controller

4.1.1 Leader UAV Control Formulation

Before deriving any control scheme, the following assumptions are made:

Assumption 4: the following condition is true for the uncertainty terms:

$\|D_{Xi}\| \leqslant \Delta_{1i}$; $\|D_{Yi}\| \leqslant \Delta_{2i}$; $\|D_{Zi}\| \leqslant \Delta_{3i}$; $\|D_{\phi_i}\| \leqslant \Delta_{4i}$; $\|D_{\theta_i}\| \leqslant \Delta_{5i}$; $\|D_{\psi_i}\| \leqslant \Delta_{6i}$

where, $\Delta_{1i}, \Delta_{2i}, \Delta_{3i}, \Delta_{4i}, \Delta_{5i}, \Delta_{6i}$ denotes the upper bound of the uncertainties.

In this section, considering [38] using the adaptive super twisting sliding mode control method the attitude, altitude, and position controllers are designed.

4.1.1.1 Attitude Control

For the leader UAV, let the desired Euler angle commands be set as $\phi_{dL}, \theta_{dL}, \psi_{dL}$, then accordingly to these desired commands let the phi desired sliding manifold:

$$S_{\phi_L} = k_1 e_{\phi_L} + k_2 \dot{e_{\phi_L}} \tag{4.1}$$

where, S_{ϕ_L}, k_1, k_2 and ϕ_L denotes the sliding surface, design constants and loop error dynamics for ϕ_L loop. Where $e_{\phi_L} = \phi_L - \phi_{dL}, \dot{e_{\phi_L}} = \dot{\phi_L} - \dot{\phi_{dL}}$. Taking First order derivative with respect to time of Eq. 4.1 results in,

$$\dot{S_{\phi_L}} = k_1 \dot{e_{\phi_L}} + k_2 \ddot{e_{\phi_L}} \tag{4.2}$$

After combining Eq. 4.2 and 3.14 expressed as follows:

$$\dot{S_{\phi_L}} = k_1 \dot{e_{\phi_L}} + k_2 \left[\frac{I_{yL} - I_{zL}}{I_{xL}} \dot{\theta_L} \dot{\psi_L} + U_{2L} \frac{l_L}{I_{xL}} - \frac{J_{rL}}{I_{xL}} \dot{\theta_L} \Omega_{rL} - D_{\phi_L} - \ddot{\phi_{dL}} \right] \tag{4.3}$$

Let $a_{1L} = \frac{I_{yL} - I_{zL}}{I_{xL}}, a_{2L} = \frac{J_{rL}}{I_{xL}}, b_{1L} = \frac{l_L}{I_{xL}}$, then Eq. 4.3 becomes:

$$\dot{S_{\phi_L}} = k_1 \dot{e_{\phi_L}} + k_2 \left[a_{1L} \dot{\theta_L} \dot{\psi_L} + U_{2L} b_{1L} - a_{2L} \dot{\theta_L} \Omega_{rL} - D_{\phi_L} - \ddot{\phi_{dL}} \right] \tag{4.4}$$

Then the equivalent and switching control law using the super twisting algorithm for the ϕ_L loop is shown below:

$$U_{2Le} = \frac{1}{b_{1L}} \left(\frac{-k_1}{k_2} \dot{e_{\phi_L}} - a_{1L} \dot{\theta_L} \dot{\psi_L} + a_{2L} \dot{\theta_L} \Omega_{rL} + \ddot{\phi_{dL}} \right) \tag{4.5}$$

$$U_{2Ls} = -\frac{k_{s1}}{b_{1L}}|S_{\phi_L}|^{0.5} sgn(S_{\phi_L}) - \frac{k_{s2}}{b_{1L}} \int sgn(S_{\phi_L}) \tag{4.6}$$

From Eq. 4.5 and 4.6, the total control action leads to the following expression:

$$U_{2L} = U_{2Le} + U_{2Ls} \tag{4.7}$$

Similarly, θ_L and ψ_L loops the sliding surfaces for pitch and yaw controllers are defined as follows:

$$S_{\theta_L} = k_3 e_{\theta_L} + k_4 \dot{e_{\theta_L}} \tag{4.8}$$

$$S_{\psi_L} = k_5 e_{\psi_L} + k_6 \dot{e_{\psi_L}} \tag{4.9}$$

Now for Eq. 4.8 and 4.9 working for controller is shown below:

$$U_{3Le} = \frac{1}{b_{2L}} \left(\frac{-k_3}{k_4} \dot{e_{\theta_L}} - a_{3L} \dot{\phi_L} \dot{\psi_L} + a_{4L} \dot{\phi_L} \Omega_{rL} + \ddot{\theta_{dL}} \right) \tag{4.10}$$

$$U_{3Ls} = -\frac{k_{s3}}{b_{2L}}|S_{\theta_L}|^{0.5} sgn(S_{\theta_L}) - \frac{k_{s4}}{b_{2L}} \int sgn(S_{\theta_L}) \tag{4.11}$$

$$U_{4Le} = \frac{1}{b_{3L}} \left(\frac{-k_5}{k_6} \dot{e_{\psi_L}} - a_{5L} \dot{\phi_L} \dot{\theta_L} + \ddot{\psi_{dL}} \right) \tag{4.12}$$

$$U_{4Ls} = -\frac{k_{s5}}{b_{3L}}|S_{\psi_L}|^{0.5} sgn(S_{\psi_L}) - \frac{k_{s6}}{b_{3L}} \int sgn(S_{\psi_L}) \tag{4.13}$$

Where, $a_{3L} = \frac{I_{zL} - I_{xL}}{I_{yL}}, a_{4L} = \frac{J_{rL}}{I_{yL}}, b_{2L} = \frac{lL}{I_{yL}}, a_{5L} = \frac{I_{xL} - I_{yL}}{I_{zL}}, b_{3L} = \frac{lL}{I_{xL}}$, and $k_1, k_2, k_3, k_4, k_5, k_6, k_{s1}, k_{s2}, k_{s3}, k_{s4}, k_{s5}, k_{s6}$ denotes controllers and sliding surface gains. Also,

error dynamics for θ_L and ψ_L loops are defined as, $e_{\theta_L} = \theta_L - \theta_{dL}$, $e_{\dot{\theta}_L} = \dot{\theta_L} - \dot{\theta_{dL}}$, $e_{\psi_L} = \psi - \psi_{dL}$, $e_{\dot{\psi}_L} = \dot{\psi_L} - \dot{\psi_{dL}}$.

Theorem 1. *Attitude dynamics states in Eq. 3.14-3.16 will coincide to the origin in finite time [39] using proposed controllers of Eq. 4.5-4.13.*

Proof. Accordingly to theorem 1, stability proof of ϕ_L is derived.

The same procedures can also be used for the other two attitude dynamics θ_L and ψ_L. Eq. 4.6 can also be adjust accordingly to this equation:

$$U_{2Ls} = -\frac{k_{s1}}{b_{1L}}|S_{\phi L}|^{0.5} sgn(S_{\phi L}) + v_{\phi L} \tag{4.14}$$

As, v_{ϕ_L} is composed from the following equation: $\dot{v_{\phi_L}} = \frac{k_{s2}}{b_{1L}} sgn(S_{\phi_L})$. By merging Eq. 4.14 and 4.5 into 4.4 results into following expression:

$$\dot{S_{\phi_L}} = -\frac{k_{s1}}{b_{1L}}|S_{\phi_L}|^{0.5} sgn(S_{\phi_L}) + v_{\phi_L} - D_{\phi_L} \tag{4.15}$$

$$\dot{v_{\phi_L}} = \frac{k_{s2}}{b_{1L}} sgn(S_{\phi_L}) \tag{4.16}$$

For ϕ loop dynamics let the Lyapunov function :

$$V_{\phi_L} = 2\lambda_2|S_{\phi_L}| + 0.5{v_{\phi_L}}^2 + 0.5\left(\lambda_1|S_{\phi_L}|^{0.5} sgn(S_{\phi_L}) - v_{\phi_L}\right)^2 \tag{4.17}$$

Where, $\lambda_1 = \frac{k_{s1}}{b_{1L}}$ and $\lambda_2 = \frac{k_{s2}}{b_{1L}}$.

New state vector is defined as follows: ${\eta_{\phi_L}}^T = \begin{bmatrix} |S_{\phi_L}|^{0.5} sgn(S_{\phi_L}) & v_{\phi_L} \end{bmatrix}$. Defining Matrix $P_{\phi_L} = \begin{bmatrix} 4\lambda_2 + \lambda^2 & -\lambda \\ -\lambda & 2 \end{bmatrix}$ and then the Lyapunov function is modified as follows: $V_{\phi_L} = {\eta_{\phi_L}}^T P \eta_{\phi_L}$. First order derivative with respect to time of the Lyapunov function with Eq. 4.16 formulates the following expression:

$$\dot{V_{\phi_L}} = -\frac{1}{|S_{\phi_L}|^{0.5}} {\eta_{\phi_L}}^T Q \eta_{\phi_L} + \Delta_{4L} {q_{\phi_L}}^T \eta_{\phi_L} \tag{4.18}$$

Where, $Q_{\phi_L} = \frac{\lambda_1}{2} \begin{bmatrix} 2\lambda_2 + {\lambda_1}^2 & -\lambda_1 \\ -\lambda_1 & 1 \end{bmatrix}$ and ${q_{\phi_L}}^T = \left(2\lambda_2 + \frac{1}{2}{\lambda_1}^2 - \frac{1}{2}\lambda_1\right)$. Under considering assumption 4 Eq. 4.18 will be simplified as follows:

$$\dot{V_{\phi_L}} = -\frac{\lambda_1}{2|S_{\phi_L}|^{0.5}} {\eta_{\phi_L}}^T {Q_{\phi_L}}^{\frown} \eta_{\phi_L} \tag{4.19}$$

Where, ${Q_{\phi_L}}^{\frown} = \begin{bmatrix} 2\lambda_2 + {\lambda_1}^2 - \left(\frac{4\lambda_2}{\lambda_1} + \lambda_1\right)\Delta_{4L} & -\lambda_1 + 2\Delta_{4L} \\ -\lambda_1 + 2\Delta_{4L} & 1 \end{bmatrix}$. If ${Q_{\phi_L}}^{\frown} > 0$ then Eq. 4.19 is negative definite, also if $\lambda_1 > 2\Delta_{4L}$, $\lambda_2 > \lambda_1 \frac{5\Delta_{4L}\lambda_1 + 4{\Delta_{4L}}^2}{2(\lambda_1 - 2\Delta_{4L})}$, then $Q^{\frown} > 0$ and $\dot{V_{\phi_L}} < 0$.

Remark 1. *Using procedures adopted in [39] A proof of the convergent nature can be obtained in a finite amount of time.*

4.1.1.2 Altitude and Position Control

Initially, the UAV quad-copter altitude control system is derived, then using a transformation matrix the position controllers are calculated. The sliding manifold for the desired altitude Z_{dL} is expressed below:

$$S_{Z_L} = k_7 e_{Z_L} + k_8 \dot{e_{Z_L}} \tag{4.20}$$

Where, k_7 and k_8 depicts the design constants. The error calculated is as follows: $e_{Z_L} = Z_L - Z_{dL}$, $\dot{e_{Z_L}} = \dot{Z_L} - \dot{Z_{dL}}$. Taking the first order derivative with respect to time of Eq. 4.20 leads to the following equation:

$$\dot{S_{Z_L}} = k_7 \dot{e_{Z_L}} + k_8 \ddot{e_{Z_L}} \tag{4.21}$$

Merging Eq. 4.21 and 3.13 gives us:

$$\dot{S_{Z_L}} = k_7 \dot{e_{Z_L}} + k_8 \left[g - U_{1L}(\cos\theta_L \cos\phi_L)\frac{1}{m_{QL}} - D_{ZL} - \ddot{Z_{dL}} \right] \tag{4.22}$$

Making use of the super twisting SMC theory, the leader UAV altitude controller is formulated as below:

$$U_{Z_L} = -\frac{k_7}{k_8}\dot{e_{Z_L}} + \ddot{Z_{dL}} - \frac{k_{s7}}{k_8}|S_{Z_L}|^{0.5} sgn(S_{Z_L}) - \frac{k_{s8}}{k_8}\int sgn(S_{Z_L}) \tag{4.23}$$

$$U_{1L} = \frac{m_{QL}}{\cos\theta_L \cos\phi_L}\left[g - \left(-\frac{k_7}{k_8}\dot{e_{Z_L}} + \ddot{Z_{dL}} - \frac{k_{s7}}{k_8}|S_{Z_L}|^{0.5} sgn(S_{Z_L}) - \frac{k_{s8}}{k_8}\int sgn(S_{Z_L}) \right) \right] \tag{4.24}$$

Where, $U_{Z_L} = \ddot{Z_L} = g - (\cos\theta_L \cos\phi_L)\frac{U_{1L}}{m_{QL}}$ represents the virtual control law. Using the same concepts presented for the ϕ loop, altitude stability proof is derived. To derive the XY controllers, let:

$$U_{XL} = U_{1L}(\sin\psi_L \sin\phi_L + \cos\psi_L \sin\theta_L \cos\phi_L)\frac{1}{m_{QL}} \tag{4.25}$$

$$U_{YL} = U_{1L}(-\cos\psi_L \sin\phi_L + \sin\psi_L \sin\theta_L \cos\phi_L)\frac{1}{m_{QL}} \tag{4.26}$$

Eq. 3.11 and 3.12 are altered for the leader UAV which are expressed below:

$$\ddot{X_L} = U_{XL} - D_{XL} \tag{4.27}$$

$$\ddot{Y_L} = U_{YL} - D_{YL} \tag{4.28}$$

Sliding manifolds for the leader UAV position loop can be expressed in the following form:

$$S_{X_L} = k_9 e_{X_L} + k_{10} \dot{e_{X_L}} \tag{4.29}$$

$$S_{Y_L} = k_{11} e_{Y_L} + k_{12} \dot{e_{Y_L}} \tag{4.30}$$

Where, $k_9, k_{10}, k_{11}, k_{12}$ denotes the design constants and the error dynamics are expressed as follows: $e_{X_L} = X_L - X_{dL}$, $\dot{e_{X_L}} = \dot{X_L} - \dot{X_{dL}}$, $e_{Y_L} = Y_L - Y_{dL}$, $\dot{e_{Y_L}} = \dot{Y_L} - \dot{Y_{dL}}$. Taking first order derivative with respect to time of Eq. 4.29 and 4.30, then combining it with Eq. 4.27 and 4.28 formulates to following equation:

$$\dot{S_{X_L}} = k_9 \dot{e_{X_L}} + k_{10}[U_{XL} - D_{XL} - \ddot{X_{dL}}] \tag{4.31}$$

$$\dot{S_{Y_L}} = k_{11} \dot{e_{Y_L}} + k_{12}[U_{YL} - D_{YL} - \ddot{Y_{dL}}] \tag{4.32}$$

From Eq. 4.31 and 4.32 following virtual controllers U_{XL} and U_{YL} are derived:

$$U_{XL} = \left(\ddot{X_{dL}} - \frac{k_9}{k_{10}} \dot{e_{X_L}} - \frac{k_{s9}}{k_{10}} |S_{X_L}|^{0.5} sgn(S_{X_L}) - \frac{k_{s10}}{k_{10}} \int sgn(S_{X_L}) \right) \tag{4.33}$$

$$U_{YL} = \left(\ddot{Y_{dL}} - \frac{k_{11}}{k_{12}} \dot{e_{Y_L}} - \frac{k_{s11}}{k_{12}} |S_{Y_L}|^{0.5} sgn(S_{Y_L}) - \frac{k_{s12}}{k_{12}} \int sgn(S_{Y_L}) \right) \tag{4.34}$$

Using same concepts presented for ϕ loop, the $\dot{S_{X_L}}$ and $\dot{S_{Y_L}}$ are expressed as following:

$$\dot{S_{X_L}} = -\frac{k_{s9}}{k_{10}} |S_{X_L}|^{0.5} sgn(S_{X_L}) + v_{X_L} - D_{XL} \tag{4.35}$$

$$\dot{v_{X_L}} = \frac{k_{s10}}{k_{10}} sgn(S_{X_L}) \tag{4.36}$$

$$\dot{S_{Y_L}} = -\frac{k_{s11}}{k_{12}} |S_{Y_L}|^{0.5} sgn(S_{Y_L}) + v_{Y_L} - D_{YL} \tag{4.37}$$

$$\dot{v_{Y_L}} = \frac{k_{s12}}{k_{12}} sgn(S_{Y_L}) \tag{4.38}$$

Where, $\dot{v_{X_L}} = -\frac{k_{s10}}{k_{10}} sgn(S_{X_L})$, and $\dot{v_{Y_L}} = -\frac{k_{s11}}{k_{12}} sgn(S_{Y_L})$. For X and Y loop dynamics let the Lyapunov functions be:

$$V_{X_L} = \frac{1}{2} {v_{X_L}}^2 + 2\lambda_{10} |S_{X_L}| + \frac{1}{2} \left(\lambda_9 |S_{X_L}|^{0.5} sgn(S_{X_L}) - v_{X_L} \right)^2 \tag{4.39}$$

$$V_{Y_L} = \frac{1}{2} {v_{Y_L}}^2 + 2\lambda_{12} |S_{Y_L}| + \frac{1}{2} \left(\lambda_{11} |S_{Y_L}|^{0.5} sgn(S_{Y_L}) - v_{Y_L} \right)^2 \tag{4.40}$$

Where, $\lambda_9 = \frac{k_{s9}}{k_{10}}$, $\lambda_{10} = \frac{k_{s10}}{k_{10}}$, $\lambda_{11} = \frac{k_{s11}}{k_{12}}$, $\lambda_{12} = \frac{k_{s12}}{k_{12}}$. The new state vectors can be defined as follows: ${\eta_{XL}}^T = \begin{bmatrix} |S_{X_L}|^{0.5} sgn(S_{X_L}) & v_{X_L} \end{bmatrix}$; ${\eta_{YL}}^T = \begin{bmatrix} |S_{Y_L}|^{0.5} sgn(S_{Y_L}) & v_{Y_L} \end{bmatrix}$. Following creative matrices are defined as: $P_{XL} = \begin{bmatrix} 4\lambda_{10} + {\lambda_9}^2 & -\lambda_9 \\ -\lambda_9 & 2 \end{bmatrix}$; $P_{YL} = \begin{bmatrix} 4\lambda_{12} + {\lambda_{11}}^2 & -\lambda_{11} \\ -\lambda_{11} & 2 \end{bmatrix}$ and then the Lyapunov function is modified as follows: $V_{X_L} = \zeta_1 {\eta_{XL}}^T P_{XL} \eta_{XL} + {D_{XL}}^T D_{XL}$; $V_{Y_L} = \zeta_2 {\eta_{YL}}^T P_{YL} \eta_{YL} + {D_{YL}}^T D_{YL}$. First order derivative with respect to time of the Lyapunov function along Eq. 4.35-4.38 yields the following relation [45]:

$$\dot{V_{X_L}} = -\zeta_1 \frac{1}{|S_{X_L}|^{0.5}} {\eta_{XL}}^T Q_{XL} \eta_{XL} + \zeta_1 D_{XL} {q_{XL}}^T \eta_{XL} + {D_{XL}}^T \dot{D_{XL}} \tag{4.41}$$

$$\dot{V_{Y_L}} = -\zeta_2 \frac{1}{|S_{Y_L}|^{0.5}} {\eta_{YL}}^T Q_{YL} \eta_{YL} + \zeta_2 D_{YL} {q_{YL}}^T \eta_{YL} + {D_{YL}}^T \dot{D_{YL}} \tag{4.42}$$

Where $Q_{XL} = \frac{\lambda_9}{2}\begin{bmatrix} 2\lambda_{10} + {\lambda_9}^2 & -\lambda_9 \\ -\lambda_9 & 1 \end{bmatrix}$; $Q_{YL} = \frac{\lambda_{11}}{2}\begin{bmatrix} 2\lambda_{12} + {\lambda_{11}}^2 & -\lambda_{11} \\ -\lambda_{11} & 1 \end{bmatrix}$ and ${q_{XL}}^T = (2\lambda_{10} + \frac{1}{2}{\lambda_9}^2 - \frac{1}{2}\lambda_9)$; ${q_{YL}}^T = (2\lambda_{12} + \frac{1}{2}{\lambda_{11}}^2 - \frac{1}{2}\lambda_{11})$. As D_{XL} and D_{YL} are scalar quantities so ${D_{XL}}^T = D_{XL}$ and ${D_{YL}}^T = D_{YL}$, then adaptive laws are formulated:

$$\dot{D_{XL}} = -\zeta_1 {q_{XL}}^T \eta_{XL} \tag{4.43}$$

$$\dot{D_{YL}} = -\zeta_2 {q_{YL}}^T \eta_{YL} \tag{4.44}$$

Where, ζ_1 and ζ_2 denotes the adaptation gains. Accordingly to Assumption 4, and by combining Eq. 4.41-4.42 with Eq. 4.43-4.44 yields the following simplified expressions as follows [39]:

$$\dot{V_{XL}} = -\frac{\lambda_9}{2|S_{X_L}|^{0.5}} {\eta_{XL}}^T {Q_{XL}}^{\frown} \eta_{XL} \tag{4.45}$$

$$\dot{V_{YL}} = -\frac{\lambda_{11}}{2|S_{Y_L}|^{0.5}} {\eta_{YL}}^T {Q_{XL}}^{\frown} \eta_{YL} \tag{4.46}$$

Where ${Q_{XL}}^{\frown} = \begin{bmatrix} 2\lambda_{10} + {\lambda_9}^2 - \left(\frac{4\lambda_{10}}{\lambda_9} + \lambda_9\right) E\Delta_{1L} & -\lambda_9 + 2E\Delta_{1L} \\ -\lambda_9 + 2E\Delta_{1L} & 1 \end{bmatrix}$ and ${Q_{YL}}^{\frown} = \begin{bmatrix} 2\lambda_{12} + {\lambda_{11}}^2 - \left(\frac{4\lambda_{12}}{\lambda_{11}} + \lambda_{11}\right) E\Delta_{2L} & -\lambda_{11} + 2E\Delta_{2L} \\ -\lambda_{11} + 2E\Delta_{2L} & 1 \end{bmatrix}$. $\dot{V_{XL}}$ and $\dot{V_{YL}}$ are negative definite only if ${Q_{XL}}^{\frown} > 0$ and ${Q_{YL}}^{\frown} > 0$. If gains satisfy the following criteria $\lambda_9 > 2E\Delta_{1L}$, $\lambda_{10} > \lambda_9 \frac{5E\Delta_{1L}\lambda_9 + 4{E\Delta_{1L}}^2}{2(\lambda_9 - 2E\Delta_{1L})}$; $\lambda_{11} > 2E\Delta_{2L}$, $\lambda_{12} > \lambda_{11} \frac{5E\Delta_{2L}\lambda_{11} + 4{E\Delta_{2L}}^2}{2(\lambda_{11} - 2E\Delta_{2L})}$, then ${Q_{XL}}^{\frown} > 0$; ${Q_{YL}}^{\frown} > 0$ and $\dot{V_{XL}} < 0$; $\dot{V_{YL}} < 0$. Where $E\Delta_{1L} = D_{XL_{estimated}} - D_{XL}$ and $E\Delta_{2L} = D_{YL_{estimated}} - D_{YL}$ denotes the estimation error of the adaptive loops.

U_{XL} and U_{YL} are the virtual controllers for the desired reference trajectories of ϕ_{dl} and θ_{dl}:

$$\frac{U_{XL}m_{QL}}{U_{1L}} = \cos\psi_L \sin\theta_L \cos\phi_L + \sin\phi_L \sin\psi_L \tag{4.47}$$

$$\frac{U_{YL}m_{QL}}{U_{1L}} = \sin\psi_L \sin\theta_L \cos\phi_L - \sin\phi_L \cos\psi_L \tag{4.48}$$

Multiplying Eq. 4.47 with $\sin\psi$ and Eq. 4.48 with $\cos\psi$, then the difference between the obtained equations leads to the following equation:

$$\frac{U_{XL}m_{QL}}{U_{1L}} \sin\psi - \frac{U_{YL}m_{QL}}{U_{1L}} \cos\psi = \sin\phi_{dL} \tag{4.49}$$

From Eq. 4.49 the reference command for ϕ loop as follows:

$$\phi_{dL} = \sin^{-1}\left[\frac{U_{XL}m_{QL}}{U_{1L}} \sin\psi - \frac{U_{YL}m_{QL}}{U_{1L}} \cos\psi\right] \tag{4.50}$$

Multiplying Eq. 4.47 with $\cos\psi$ and Eq. 4.48 by $\sin\psi$, then adding the resulting equations formulates to the following equation:

$$\frac{U_{XL}m_{QL}}{U_{1L}} \cos\psi + \frac{U_{YL}m_{QL}}{U_{1L}} \sin\psi = \sin\theta_{dL} \cos\phi_L \tag{4.51}$$

Squaring Eq. 4.49 and putting $\sin{\phi_L}^2 = 1 - \cos{\phi_L}^2$ formulate to the following equation:

$$\cos\phi_{dL} = \sqrt{1 - \left[\frac{U_{XL}m_{QL}}{U_{1L}} \sin\psi - \frac{U_{YL}m_{QL}}{U_{1L}} \cos\psi\right]^2} \tag{4.52}$$

Putting Eq. 4.52 in Eq. 4.51 formulates the reference command for θ loop:

$$\theta_{dL} = \sin^{-1}\left[\frac{\frac{U_{XL}m_{QL}}{U_{1L}}\cos\psi \ + \frac{U_{YL}m_{QL}}{U_{1L}}\sin\psi}{\sqrt{1-\left[\frac{U_{XL}m_{QL}}{U_{1L}}\sin\psi - \frac{U_{YL}m_{QL}}{U_{1L}}\cos\psi\right]^2}}\right] \tag{4.53}$$

4.1.2 Leader Followers Formation Control

The sliding surface for the required trajectory of the followers' UAVs can be formulated as follows:

$$S_{X_f} = X_f + \lambda \int X_f \tag{4.54}$$

Where λ denotes the sliding surface gain matrix. Taking first order derivative with respect to time of Eq. 4.54 and combining it with Eq. 3.24 yields the following expression:

$$\dot{S_{X_f}} = F(X_f) + G(X_f)v_f + \lambda X_f \tag{4.55}$$

The followers' UAVs desired lateral and longitudinal velocities are formulated as follows:

$$v_{f_e} = G(X_f)^{-1}[-F(X_f) - \lambda X_f] \tag{4.56}$$

$$v_{f_s} = -\eta_1 |S_{X_f}|^{0.5} sgn(S_{X_f}) - \eta_2 \int sgn(S_{X_f}) \tag{4.57}$$

To ensure stability, the same procedure as for the attitude loops is applied here.

4.1.3 Followers UAV Controllers Formulation

As the reference position trajectories are generated by Eq. 3.27 and 3.28 then governed by the formation controller mentioned in Eq. 4.56 and 4.57. For the rest of the followers' UAVs, the analysis and derivation are the same as the leader UAV. Simplified endmost control laws are mentioned, let the sliding manifolds for attitude be expressed as follows:

$$S_{\phi_f} = k_{1f} e_{\phi_f} + k_{2f} \dot{e_{\phi_f}} \tag{4.58}$$

$$S_{\theta_f} = k_{3f} e_{\theta_f} + k_{4f} \dot{e_{\theta_f}} \tag{4.59}$$

$$S_{\psi_f} = k_{5f} e_{\psi_f} + k_{6f} \dot{e_{\psi_f}} \tag{4.60}$$

Where, $f = [F_1, F_2]$ as F_1 and F_2 represents the follower 1 and follower 2 UAVs respectively. Also k_{1f}, k_{2f}, k_{3f}, k_{4f}, k_{5f}, k_{6f} denotes the sliding surface design constants for followers UAV. Where $e_{\phi_f} = \phi_f - \phi_{df}$; $e_{\theta_f} = \theta_f - \theta_{df}$; $e_{\psi_f} = \psi_f - \psi_{df}$. Similarly attitude and position sliding manifolds are expressed as follows:

$$S_{Z_f} = k_{7f} e_{Z_f} + k_{8f} \dot{e_{Z_f}} \tag{4.61}$$

$$S_{X_f} = k_{9f} e_{X_f} + k_{10f} \dot{e_{X_f}} \tag{4.62}$$

$$S_{Y_f} = k_{11f} e_{Y_f} + k_{12f} \dot{e_{Y_f}} \tag{4.63}$$

Where, k_{7f}, k_{8f}, k_{9f}, k_{10f}, k_{11f}, k_{12f} denotes the sliding surface design constants for followers UAV. Where $e_{Z_f} = Z_f - Z_{df}$; $e_{X_f} = X_f - X_{df}$; $e_{Y_f} = Y_f - Y_{df}$. Using

the same procedures adopted for attitude, altitude, and position, controllers for the followers UAVs are formulated as follows:

$$U_{2fe} = \frac{1}{b_{1f}} \left(\frac{-k_{1f}}{k_{2f}} e_{\dot{\phi}_f} - a_{1f} \dot{\theta}_f \dot{\psi}_f + a_{2f} \dot{\theta}_f \Omega_{rf} + \ddot{\phi}_{df} \right) \tag{4.64}$$

$$U_{2fs} = -\frac{k_{s1f}}{b_{1f}} |S_{\phi f}|^{0.5} sgn(S_{\phi_f}) - \frac{k_{s2f}}{b_{1f}} \int sgn(S_{\phi_f}) \tag{4.65}$$

$$U_{3fe} = \frac{1}{b_{2f}} \left(\frac{-k_{3f}}{k_{4f}} e_{\dot{\theta}_f} - a_{3f} \dot{\phi}_f \dot{\psi}_f + a_{4f} \dot{\phi}_f \Omega_{rf} + \ddot{\theta}_{df} \right) \tag{4.66}$$

$$U_{3fs} = -\frac{k_{s3f}}{b_{2f}} |S_{\theta_f}|^{0.5} sgn(S_{\theta_f}) - \frac{k_{s4f}}{b_{2f}} \int sgn(S_{\theta_f}) \tag{4.67}$$

$$U_{4fe} = \frac{1}{b_{3f}} \left(\frac{-k_{5f}}{k_{6f}} e_{\dot{\psi}_f} - a_{5f} \dot{\phi}_f \dot{\theta}_f + \ddot{\psi}_{df} \right) \tag{4.68}$$

$$U_{4fs} = -\frac{k_{s5f}}{b_{3f}} |S_{\psi_f}|^{0.5} sgn(S_{\psi_f}) - \frac{k_{s6f}}{b_{3f}} \int sgn(S_{\psi_f}) \tag{4.69}$$

$$U_{1f} = \frac{m_{Qf}}{\cos\theta_f \cos\phi_f} \left[g - \left(-\frac{k_{7f}}{k_{8f}} e_{\dot{Z}f} + \ddot{Z}_{df} - \frac{k_{s7f}}{k_8 f} |S_{Zf}|^{0.5} sgn(S_{Zf}) - \frac{k_{s8f}}{k_8 f} \int sgn(S_{Zf}) \right) \right] \tag{4.70}$$

$$U_{Xf} = \left(\ddot{X}_{df} - \frac{k_{9f}}{k_{10f}} e_{\dot{X}f} - \frac{k_{s9f}}{k_{10f}} |S_{Xf}|^{0.5} sgn(S_{Xf}) - \frac{k_{s10f}}{k_{10f}} \int sgn(S_{Xf}) \right) \tag{4.71}$$

$$U_{Yf} = \left(\ddot{Y}_{df} - \frac{k_{11f}}{k_{12f}} e_{\dot{Y}f} - \frac{k_{s11f}}{k_{12f}} |S_{Yf}|^{0.5} sgn(S_{Yf}) - \frac{k_{s12f}}{k_{12f}} \int sgn(S_{Yf}) \right) \tag{4.72}$$

$$\dot{D_{Xf}} = \zeta_1 f S_{X_f} \tag{4.73}$$

$$\dot{D_{Yf}} = \zeta_2 f S_{Y_f} \tag{4.74}$$

$$\phi_{df} = \sin^{-1}\left[\frac{U_{Xf} m_{Qf}}{U_{1f}}\sin\psi - \frac{U_{Yf} m_{Qf}}{U_{1f}}\cos\psi\right] \tag{4.75}$$

$$\theta_{df} = \sin^{-1}\left[\frac{\frac{U_{Xf} m_{Qf}}{U_{1f}}\cos\psi + \frac{U_{Yf} m_{Qf}}{U_{1f}}\sin\psi}{\sqrt{1 - \left[\frac{U_{Xf} m_{Qf}}{U_{1f}}\sin\psi - \frac{U_{Yf} m_{Qf}}{U_{1f}}\cos\psi\right]^2}}\right] \tag{4.76}$$

4.2 Integral Backstepping Controller

In this section, we will formulate the integral backstepping controller only on the position controller to check the robustness of the controller. To easily implement a backstepping control strategy, the acquired mathematical model is converted into the state space form:

$$\dot{X}_i = f(X_i, U_i) \tag{4.77}$$

Where, i is an index representing $[L, f]$, as $f = [F1, F2]$. The subscript L denotes the Leader UAV, while $F1$ and $F2$ denote Follower 1 and 2 respectively. Here, X_i, U_i denotes the state vector and input vector.

$$X_i = \left[\phi_i \;\; \dot{\phi}_i \;\; \theta_i \;\; \dot{\theta}_i \;\; \psi_i \;\; \dot{\psi}_i \;\; z_i \;\; \dot{z}_i \;\; x_i \;\; \dot{x}_i \;\; y_i \;\; \dot{y}_i\right]^T \tag{4.78}$$

State vector can also be written as:

$$X_i = [x_{1i} \;\; x_{2i} \;\; x_{3i} \;\; x_{4i} \;\; x_{5i} \;\; x_{6i} \;\; x_{7i} \;\; x_{8i} \;\; x_{9i} \;\; x_{10i} \;\; x_{11i} \;\; x_{12i}] \tag{4.79}$$

Where control inputs cn be written as:

$$U_i = [U_{1i} \;\; U_{2i} \;\; U_{3i} \;\; U_{4i}] \tag{4.80}$$

From Eq. 4.77-4.79 and Eq. 3.11-3.16 state space model is modified as follows:

$$\dot{x_{1i}} = x_{2i} \tag{4.81}$$

$$\dot{x_{2i}} = c_{1i}x_{4i}x_{6i} - c_{2i}x_{4i}\Omega_{ri} + d_{1i}U_{2i} \tag{4.82}$$

$$\dot{x_{3i}} = x_{4i} \tag{4.83}$$

$$\dot{x_{4i}} = c_{3i}x_{2i}x_{6i} - c_{4i}x_{2i}\Omega_{ri} + d_{2i}U_{3i} \tag{4.84}$$

$$\dot{x_{5i}} = x_{6i} \tag{4.85}$$

$$\dot{x_{6i}} = c_{5i}x_{2i}x_{4i} + d_{3i}U_{4i} \tag{4.86}$$

$$\dot{x_{7i}} = x_{8i} \tag{4.87}$$

$$\dot{x_{8i}} = g - (\cos x_{3i} \cos x_{1i})\frac{U_{1i}}{m_{Qi}} \tag{4.88}$$

$$\dot{x_{9i}} = x_{10i} \tag{4.89}$$

$$\dot{x_{10i}} = (\sin x_{5i} \sin x_{1i} + \cos x_{5i} \sin x_{3i} \cos x_{1i}) \frac{U_{1i}}{m_{Qi}} \tag{4.90}$$

$$\dot{x_{11i}} = x_{12i} \tag{4.91}$$

$$\dot{x_{12i}} = (-\cos x_{5i} \sin x_{1i} + \sin x_{5i} \sin x_{3i} \cos x_{1i}) \frac{U_{1i}}{m_{Qi}} \tag{4.92}$$

Where, $c_{1i} = \frac{I_{yi}-I_{zi}}{I_{xi}}$, $c_{2i} = \frac{J_{ri}}{I_{xi}}$, $d_{1i} = \frac{l_i}{I_{xi}}$; $c_{3i} = \frac{I_{zi}-I_{xi}}{I_{yi}}$, $c_{4i} = \frac{J_{ri}}{I_{yi}}$, $d_{2i} = \frac{l_i}{I_{yi}}$; $c_{5i} = \frac{I_{xi}-I_{yi}}{I_{zi}}$, $d_{3i} = \frac{l_i}{I_{zi}}$.

4.2.1 Leader UAV Control Formulation

In this section, using the integral backstepping control method the attitude, altitude, and position controllers for leader UAVs are designed.

4.2.1.1 Attitude Control

For Eq. 4.81 and 4.82, for ϕ loop of the UAV leader let the positive definite Lyapunov function be as follows:

$$V(e_{1L}) = \frac{1}{2} {e_{1L}}^2 \tag{4.93}$$

Where, $e_{1L} = x_{1dL} - x_{1L}$. Taking first order derivative with respect to time of Eq. 4.93 yields the following expression:

$$\dot{V}(e_{1L}) = e_{1L} \dot{e_{1L}} \tag{4.94}$$

$$\dot{V}(e_{1L}) = e_{1L}(\dot{x_{1dL}} - x_{2L}) \tag{4.95}$$

The system is guaranteed to be a stable system [29] if the time derivative of a positive definite Lyapunov function is negative semi-definite accordingly to the Krsovskii-LaSalle principle. Stability of e_{1L} is obtained by virtual control input x_{2L}.

$$x_{2L} = \dot{x_{1dL}} + k_{1L}e_{1L}(k_{1L} > 0) \tag{4.96}$$

Augmented Lyapunov function is expressed as follows:

$$V(e_{1L}, e_{2L}) = \frac{1}{2}({e_{1L}}^2 + {e_{2L}}^2) \tag{4.97}$$

Where, $e_{2L} = x_{2L} - \dot{x_{1dL}} - k_{1L}e_{1L}$. Taking first order derivative with respect to time of Eq. 4.97 yields the following expression:

$$\dot{V}(e_{1L}, e_{2L}) = e_{1L}\dot{e_{1L}} + e_{2L}\dot{e_{2L}} \tag{4.98}$$

$$\dot{V}(e_{1L}, e_{2L}) = e_{1L}(\dot{x_{1dL}} - x_{2L}) + e_{2L}(\dot{x_{2L}} - \ddot{x_{1dL}} - k_{1L}\dot{e_{1L}})$$

$$\begin{aligned}\dot{V}(e_{1L}, e_{2L}) = e_{1L}(\dot{x_{1dL}} - x_{2L}) + e_{2L}[c_{1i}x_{4i}x_{6i} - c_{2i}x_{4i}\Omega_{ri} + d_{1i}U_{2i} \\ - \ddot{x_{1dL}} - k_{1L}(\dot{x_{1dL}} - \dot{x_{1L}})]\end{aligned} \tag{4.99}$$

Rearranging and using $e_{2L} + k_{1L}e_{1L} = x_{2L} - \dot{x_{1dL}}$ yields the following expression:

$$\dot{V}(e_{1L}, e_{2L}) = e_{2L}(c_{1L}x_{4L}x_{6L}+d_{1L}U_{2L}-\Omega_{rL}c_{2L}x_{4l})-e_{2l}\left(\ddot{x_{1dL}} - k_{1L}(e_{2L} + k_{1L}e_{1L})\right) - e_{1L}e_{2L} - k_{1L}{e_{1L}}^2 \quad (4.100)$$

The control input U_{2L} is derived from Eq. 4.100 satisfying $\dot{V(e_{1L}}, e_{2L}) < 0$.

$$U_{2L} = \frac{1}{d_{1L}}\left[e_{1L} - x_{4L}x_{6L}c_{1L} - x_{4L}c_{2L}\Omega_{rL} - c_{1L}(e_{2L} + k_{1L}e_{1L}) - k_{2L}e_{2L}\right] \quad (4.101)$$

Where, k_{1L}, k_{2L} are positive design constants. Similarly, the same procedure adopted for θ and ψ loop of Leader UAV, formulated controllers are expressed as below:

$$U_{3L} = \frac{1}{d_{2L}}\left[e_{3L} - x_{2L}x_{6L}c_{3L} - x_{2L}c_{4L}\Omega_{rL} - c_{3L}(e_{4L} + k_{3L}e_{3L}) - k_{4L}e_{4L}\right] \quad (4.102)$$

$$U_{4L} = \frac{1}{d_{3L}}\left[e_{5L} - x_{2L}x_{4L}c_{5L} - c_{5L}(e_{6L} + k_{5L}e_{5L}) - k_{6L}e_{6L}\right] \quad (4.103)$$

Where, $e_{3L} = x_{3dL} - x_{3L}$, $e_{4L} = x_{4L} - \dot{x_{3dL}} - k_{3L}e_{3L}$; $e_{5L} = x_{5dL} - x_{5L}$, $e_{6L} = x_{6L} - \dot{x_{5dL}} - k_{5L}e_{5L}$. Also k_{3L}, k_{4L}, k_{5L}, k_{6L} are positive design constants.

4.2.1.2 Altitude and Position Control

The altitude control system is derived first, then position controllers are formulated using a transformation matrix. For Eq. 4.87 and 4.88, for desired altitude of the UAV leader let the positive definite Lyapunov function be as follows:

$$V(e_{7L}) = \frac{1}{2}{e_{7L}}^2 \tag{4.104}$$

Where, $e_{7L} = x_{7dL} - x_{7L}$. Taking first order derivative with respect to time of Eq. 4.104 yields the following expression:

$$\dot{V}(e_{7L}) = e_{7L}\dot{e_{7L}} \tag{4.105}$$

$$\dot{V}(e_{7L}) = e_{7L}(\dot{x_{7dL}} - x_{8L}) \tag{4.106}$$

The system is guaranteed to be a stable system [29] if the time derivative of a positive definite Lyapunov function is negative semi-definite accordingly to the Krsovskii-LaSalle principle. Stability of e_{7L} is obtained by virtual control input x_{8L}.

$$x_{8L} = \dot{x_{7dL}} + k_{7L}e_{7L}(k_{7L} > 0) \tag{4.107}$$

Augmented Lyapunov function is expressed as follows:

$$V(e_{7L}, e_{8L}) = \frac{1}{2}({e_{7L}}^2 + {e_{8L}}^2) \tag{4.108}$$

Where, $e_{8L} = x_{8L} - \dot{x_{7dL}} - k_{7L}e_{7L}$. Taking first order derivative with respect to time of Eq. 4.108 yields the following expression:

$$\dot{V}(e_{7L}, e_{8L}) = e_{7L}\dot{e_{7L}} + e_{8L}\dot{e_{8L}} \tag{4.109}$$

$$\dot{V}(e_{7L}, e_{8L}) = e_{7L}(\dot{x_{7dL}} - x_{8L}) + e_{8L}(\dot{x_{8L}} - \ddot{x_{7dL}} - k_{7L}\dot{e_{7L}})$$

$$\dot{V}(e_{7L}, e_{8L}) = e_{7L}(\dot{x_{7dL}} - x_{8L}) + e_{8L}[g - (\cos x_{3L} \cos x_{1L})\frac{U_{1L}}{m_{QL}} - \ddot{x_{7dL}} - k_{7L}(\dot{x_{7dL}} - \dot{x_{7L}})] \quad (4.110)$$

Rearranging and using $e_{8L} + k_{7L}e_{7L} = x_{7L} - \dot{x_{7dL}}$ yields the following expression:

$$\dot{V}(e_{7L}, e_{8L}) = e_{8L}\left((\cos x_{3L} \cos x_{1L})\frac{U_{1L}}{m_{QL}}\right) - e_{8L}\left(\ddot{x_{7dL}} - k_{7L}(-e_{8L} - k_{7L}e_{7L})\right) - e_{7L}e_{8L} - k_{7L}{e_{7L}}^2 \quad (4.111)$$

The control input U_{1L} is derived from Eq. 4.111 satisfying $\dot{V}(\dot{e_{7L}}, e_{8L}) < 0$.

$$U_{1L} = \frac{m_{QL}}{\cos x_{3L} \cos x_{1L}}[-e_{7L} + g + k_{7L}(e_{8L} + k_{7L}e_{7L}) + k_{8L}e_{8L}] \quad (4.112)$$

Where, k_{7L}, k_{8L} are positive design constants. To derive the XY controllers, let:

$$U_{XL} = \sin x_{5L} \sin x_{1L} + \cos x_{5L} \sin x_{3L} \cos x_{1L} \quad (4.113)$$

$$U_{YL} = -\cos x_{5L} \sin x_{1L} + \sin x_{5L} \sin x_{3L} \cos x_{1L} \quad (4.114)$$

Modified Eq. 4.90 and 4.92 expressions as follows:

$$\dot{x_{10L}} = U_{XL}\frac{U_{1L}}{m_{Qi}} \quad (4.115)$$

$$\dot{x_{12L}} = U_{YL}\frac{U_{1L}}{m_{Qi}} \quad (4.116)$$

Using the same procedure adopted for attitude and altitude loop of Leader UAV, formulated position controllers U_{XL} and U_{YL} of Leader UAV are shown below:

$$U_{XL} = \frac{m_{QL}}{U_{1L}}[e_{9L} - k_{9L}(e_{10L} + k_{9L}e_{9L}) - k_{10L}e_{10L}] \tag{4.117}$$

$$U_{YL} = \frac{m_{QL}}{U_{1L}}[e_{11L} - k_{11L}(e_{12L} + k_{11L}e_{11L}) - k_{12L}e_{12L}] \tag{4.118}$$

Where, $e_{9L} = x_{9dL} - x_{9L}$, $e_{10L} = x_{10L} - \dot{x_{9dL}} - k_{9L}e_{9L}$; $e_{11L} = x_{11dL} - x_{11L}$, $e_{12L} = x_{12L} - \dot{x_{11dL}} - k_{11L}e_{11L}$. Also k_{9L}, k_{10L}, k_{11L}, k_{12L} are positive design constants. Modified formulated position controller Eq. 4.117 and 4.118 with integral part to enhance its robustness and stability properties are expressed as below:

$$U_{XL} = \frac{m_{QL}}{U_{1L}}[e_{9L} - k_{9L}(e_{10L} + k_{9L}e_{9L}) - k_{10L}e_{10L} - \int k_{13L}e_{10L}] \tag{4.119}$$

$$U_{YL} = \frac{m_{QL}}{U_{1L}}[e_{11L} - k_{11L}(e_{12L} + k_{11L}e_{11L}) - k_{12L}e_{12L} - \int k_{14L}e_{12L}] \tag{4.120}$$

Where, k_{13L}, k_{14L} denotes positive design constants. Reference trajectories for $\phi(x_{1dL})$ and $\theta(x_{3dL})$ can be derived as given below: Let:

$$r_\phi = e_{9L} - k_{9L}(e_{10L} + k_{9L}e_{9L}) - k_{10L}e_{10L} \tag{4.121}$$

$$r_\theta = e_{11L} - k_{11L}(e_{12L} + k_{11L}e_{11L}) - k_{12L}e_{12L} \tag{4.122}$$

Modified Eq. 4.117 and 4.118 can be written as:

$$U_{XL} = -\frac{m_{QL}}{U_{1L}} r_{\phi} \tag{4.123}$$

$$U_{YL} = -\frac{m_{QL}}{U_{1L}} r_{\theta} \tag{4.124}$$

Rearranging and putting values of U_{XL} and U_{YL} from Eq. 4.113 and 4.114:

$$[\sin x_{5L} \sin x_{1L} + \cos x_{5L} \sin x_{3L} \cos x_{1L}] \frac{U_{1L}}{m_{QL}} + r_{\phi} = 0 \tag{4.125}$$

$$[-\cos x_{5L} \sin x_{1L} + \sin x_{5L} \sin x_{3L} \cos x_{1L}] \frac{U_{1L}}{m_{QL}} + r_{\theta} = 0 \tag{4.126}$$

Multiplying Eq. 4.125 with r_{θ} and Eq. 4.126 with r_{ϕ}, then the difference between the obtained equations leads to the following expression:

$$\sin x_{1L}[U_{YL} \sin x_{5L} + U_{XL} \cos x_{5L}] = \cos x_{1L} \sin x_{3L}[U_{XL} \sin x_{5L} - U_{YL} \cos x_{5L}] \tag{4.127}$$

Multiplying Eq. 4.113 with $\cos x_{5L}$ and Eq. 4.114 with $\sin x_{5L}$, then the sum of the equations obtained gives the following expression:

$$U_{XL} \cos x_{5L} + U_{YL} \sin x_{5L} = \sin x_{3L} \cos x_{1L}[\cos {x_{5L}}^2 + \sin {x_{5L}}^2] \tag{4.128}$$

$$x_{3L} = \sin^{-1}\left[\frac{U_{XL} \cos x_{5L} + U_{YL} \sin x_{5L}}{\cos x_{1L}}\right] \tag{4.129}$$

Putting Eq. 4.129 into 4.127 yields to the following expression:

$$x_{1L} = \sin^{-1}\left[U_{XL} \sin x_{5L} - U_{YL} \cos x_{5L}\right] \tag{4.130}$$

4.2.2 Followers UAV Control Formulation

As the reference position trajectories are generated by Eq. 3.27 and 3.28 then governed by the formation controller mentioned in Eq. 4.56 and 4.57. The rest of the followers' UAVs controllers have the same derivation and analysis as same as leader UAVs. Simplified final control laws, errors, position, altitude, and attitude controllers for followers UAVs are shown below:

$$U_{2f} = \frac{1}{d_{1f}} \left[e_{1f} - x_{4f} x_{6f} c_{1f} - x_{4f} c_{2f} \Omega_{rf} - c_{1f}(e_{2f} + k_{1f} e_{1f}) - k_{2f} e_{2f} \right] \tag{4.131}$$

$$U_{3f} = \frac{1}{d_{2f}} \left[e_{3f} - x_{2f} x_{6f} c_{3f} - x_{2f} c_{4f} \Omega_{rf} - c_{3f}(e_{4f} + k_{3f} e_{3f}) - k_{4f} e_{4f} \right] \tag{4.132}$$

$$U_{4f} = \frac{1}{d_{3f}} \left[e_{5f} - x_{2f} x_{4f} c_{5f} - c_{5f}(e_{6f} + k_{5f} e_{5f}) - k_{6f} e_{6f} \right] \tag{4.133}$$

$$U_{1f} = \frac{m_{Qf}}{\cos x_{3f} \cos x_{1f}} \left[-e_{7f} + g + k_{7f}(e_{8f} + k_{7f} e_{7f}) + k_{8f} e_{8f} \right] \tag{4.134}$$

$$U_{Xf} = \frac{m_{Qf}}{U_{1f}} \left[e_{9f} - k_{9f}(e_{10f} + k_{9f} e_{9f}) - k_{10f} e_{10f} - \int k_{13f} e_{10f} \right] \tag{4.135}$$

$$U_{Yf} = \frac{m_{Qf}}{U_{1f}} \left[e_{11f} - k_{11f}(e_{12f} + k_{11f} e_{11f}) - k_{12f} e_{12f} - \int k_{14f} e_{12f} \right] \tag{4.136}$$

$$x_{3f} = \sin^{-1} \left[\frac{U_{Xf} \cos x_{5f} + U_{Yf} \sin x_{5f}}{\cos x_{1f}} \right] \tag{4.137}$$

$$x_{1f} = \sin^{-1} \left[U_{Xf} \sin x_{5f} - U_{Yf} \cos x_{5f} \right] \tag{4.138}$$

Where, $f = [F_1, F_2]$ as F_1 and F_2 represents the follower 1 and follower 2 UAVs respectively. Also $e_{1f} = x_{1df} - x_{1f}$, $e_{2f} = x_{2f} - \dot{x_{1df}} - k_{1f}e_{1f}$; $e_{3f} = x_{3df} - x_{3f}$, $e_{4f} = x_{4f} - \dot{x_{3df}} - k_{3f}e_{3f}$; $e_{5f} = x_{5df} - x_{5f}$, $e_{6f} = x_{6f} - \dot{x_{5df}} - k_{5f}e_{5f}$; $e_{7f} = x_{7df} - x_{7f}$, $e_{8f} = x_{8f} - \dot{x_{7df}} - k_{7f}e_{7f}$. Also k_{1f}, k_{2f}, k_{3f}, k_{4f}, k_{5f}, k_{6f}, k_{7f}, k_{8f}, k_{9f}, k_{10f}, k_{11f}, k_{12f}, k_{13f}, k_{14f} represents the positive design constants. The reference

4.3 Summary

It can be difficult to create a controller for a system that is under-actuated and compensates for disturbances. This chapter provides a full explanation of the design of the proposed controllers needed to manage the altitude, attitude, and position of the leader and followers UAVs. One approach to designing a controller for an under-actuated quad-copter is to use a back-stepping method. This approach involves using a recursive design process to design a controller for each subsystem of the quad-copter, starting with the outermost subsystem and working inward. At first, a controller is designed to control the attitude of the quad-copter by using the propeller speeds as inputs. Then, a controller is designed to control the angular velocity by using the attitude controller and the propeller speeds as inputs. And finally, a controller for the position of the quad-copter is designed by using the attitude and angular velocity controllers as well as the propeller speeds as inputs. Another approach to control under-actuated quad-copter is using the sliding mode control. This method uses a control law that guarantees that the system states remain within a small neighborhood of the desired equilibrium point, known as the sliding surface. In any case, both approaches require precise knowledge of the dynamics of the quad-copter and advanced control techniques such as Lyapunov stability analysis and nonlinear control. Moreover, The formation controller has also been described in depth for the leader-follower configuration.

Chapter 5

Results and Discussions

In this section, the proposed Backstepping, Integral Backstepping, and ASTSMC controllers are tested for the multiple quad-copters system. Since UAVs are identical, the UAV parameters of the leader and follower UAVs are identical and are given in Table. 5.1. ASTSMC control parameters for the leader and followers UAV are homogeneous and are given in the Table. 5.2. Similarly, Integral backstepping control parameters are also identical and are given in Table. 5.3. Formation control loop parameters and parametric uncertainties are chosen as follows: $\lambda_{F1} = \lambda_{F2} = \begin{bmatrix} 1.5 \\ 1.5 \\ 0.5 \end{bmatrix}$, $\eta_{1F1} = \eta_{1F2} = \begin{bmatrix} 0.1 \\ 0.1 \\ 0.075 \end{bmatrix}$, $\eta_{2F1} = \eta_{2F2} = \begin{bmatrix} 0.05 \\ 0.05 \\ 0.02 \end{bmatrix}$; $a_{1i} = 2.5a_{1i}$, $a_{2i} = 2.5a_{2i}$, $a_{3i} = 2.5a_{3i}$, $a_{4i} = 2.5a_{4i}$, $a_{5i} = 2.5a_{5i}$, $b_{1i} = 1.75b_{1i}$, $b_{2i} = 1.75b_{2i}$, $b_{3i} = 1.75b_{3i}$. Reference command and trajectories for the leader UAV are defined as follows: $X_{dL} = \sin t$, $Y_{dL} = \cos t$ and $Z_{dL} = t$. As it is assumed that disturbance would only be applied on the X and Y dynamics of the leader UAV and would be same for the rest of the followers UAVs. External acceleration disturbance applied on X and Y dynamics are shown at Fig. 5.1.

Fig. 5.2 shows the applied external acceleration disturbance on the leader follower UAV trajectory tracking. Fig. 5.3-5.6 shows the clear picture of the Fig. 5.2 reference trajectory tracking in 2D plane separately of each UAV. Fig. 5.6 shows the combined 2D plane view of the leader-followers reference tracking under wind

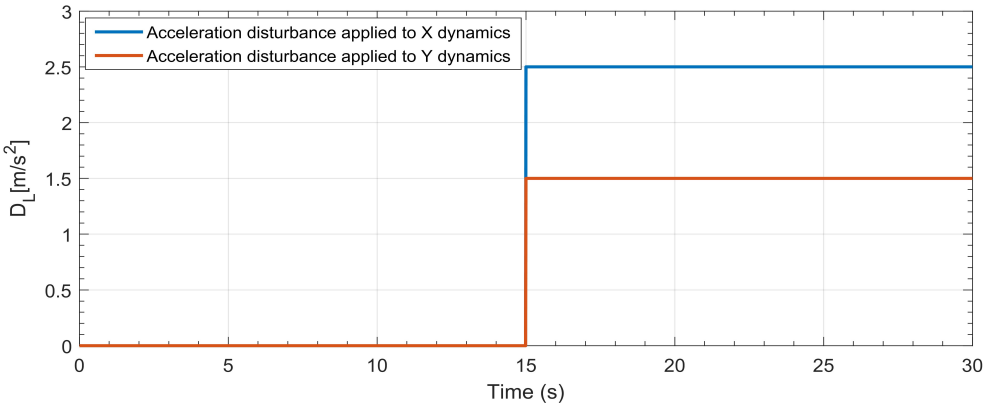

FIGURE 5.1: External acceleration disturbance applied on X and Y dynamics

TABLE 5.1: UAV Parameters for the Leader-Followers configuration

Representation	**Numerical Value**	**Unit**
$m_{QL} = m_{F1} = m_{F2}$	0.65	kg
$l_L = l_{F1} = l_{F2}$	0.23	m
$J_{rL} = J_{F1} = J_{F2}$	$6.5x10^{-5}$	$kg.m^2$
$I_{xL} = I_{xF1} = I_{xF2}$	$7.5x10^{-3}$	Ns^2rad^{-1}
$I_{yL} = I_{yF1} = I_{yF2}$	$7.5x10^{-3}$	Ns^2rad^{-1}
$I_{zL} = I_{zF1} = I_{zF2}$	$1.3x10^{-2}$	Ns^2rad^{-1}

TABLE 5.2: Leader and Followers UAV Control parameters for all loops using ASTSMC

Key Parameters	**Numerical Value**	**Key Parameters**	**Numerical Value**
k_1	200	k_2	1
k_{s1}	70	k_{s2}	15
k_3	200	k_4	1
k_{s3}	50	k_{s4}	10
k_5	95	k_6	1
k_{s5}	4.6	k_{s6}	0.5
k_7	97	k_8	1
k_{s7}	300	k_{s8}	1.5
k_9	60	k_10	1000
k_{s9}	2.5	k_{s10}	180
k_{11}	60	k_{12}	1000
k_{s11}	2.5	k_{s12}	5
η_1	1.5	η_2	2.5

TABLE 5.3: Leader and Followers UAV Control parameters for all loops using Integral Backstepping Controller

Parameter	**Value**	**Parameter**	**Value**
k_1	5	k_2	5
k_3	5	k_4	5
k_5	2	k_6	2
k_7	5	k_8	4
k_9	5	k_{10}	4
k_{11}	5	k_{12}	4
k_{13}	10	k_{14}	10

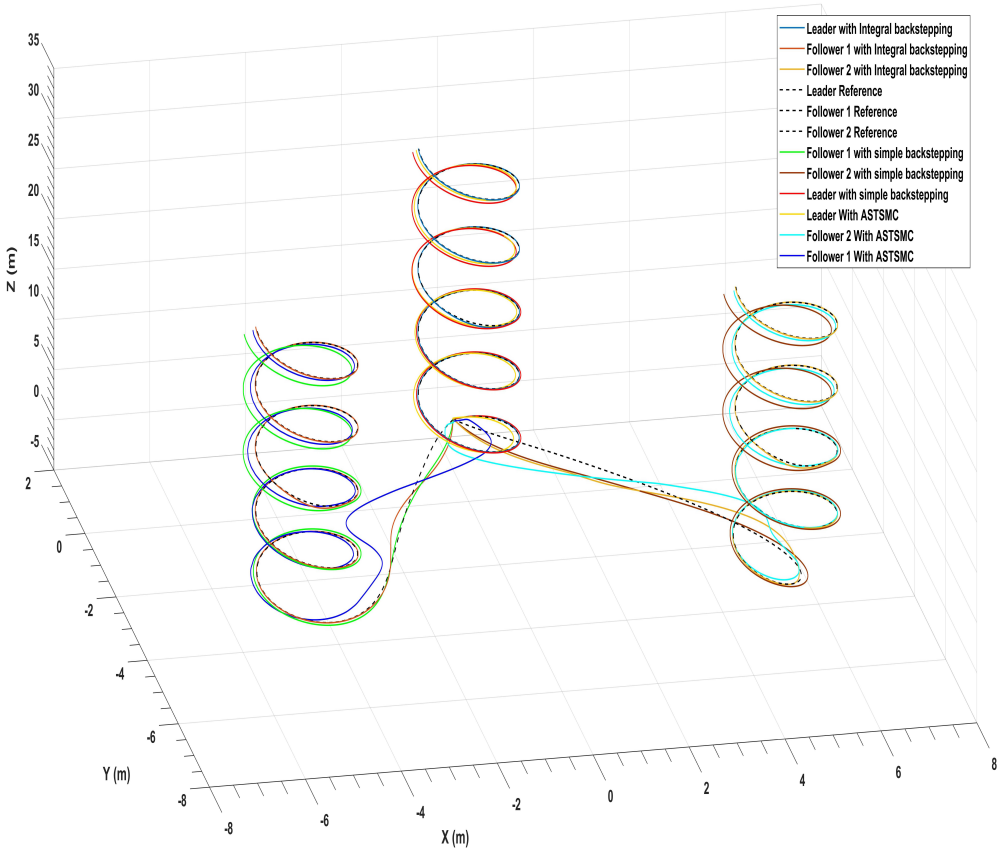

FIGURE 5.2: Trajectory tracking of XYZ under wind disturbance

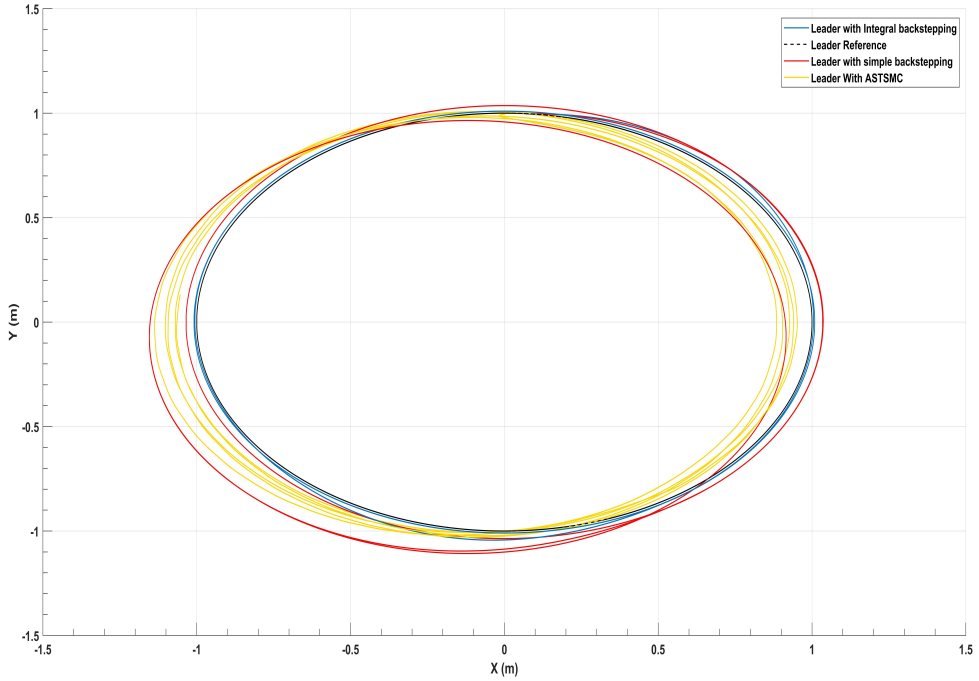

FIGURE 5.3: Trajectory tracking of Leader XY under wind disturbance

disturbances. From the outcome, it is cease that in the existence of external disturbances, the Integral backstepping controller ensures robust behavior with great performance, as the ASTSMC controller also shows good performance little slow as compared to Integral backstepping, while steady-state error is observed in a simple backstepping controller in the X and Y dynamics in the trajectory tracking characteristics of the leader and followers' UAVs.

More detailed differentiation of the UAV trajectory tracking characteristics of the preceding follower. The trajectories of X and Y are shown in Fig. 5.7 and 5.8 for the leader UAV. From Fig. 5.7, after disturbance introduced at $t = 15s$, the tracking error e_{XL} is 0.15m with the simple backstepping controller, 0.14m with ASTSMC, and 0.069m with integral backstepping controller. As integral backstepping ensures robustness and the lowest error. furthermore, suitable compensation was added by adaptive term D_{XL} of ASTSMC to neutralize the external disturbance by switching to -80.

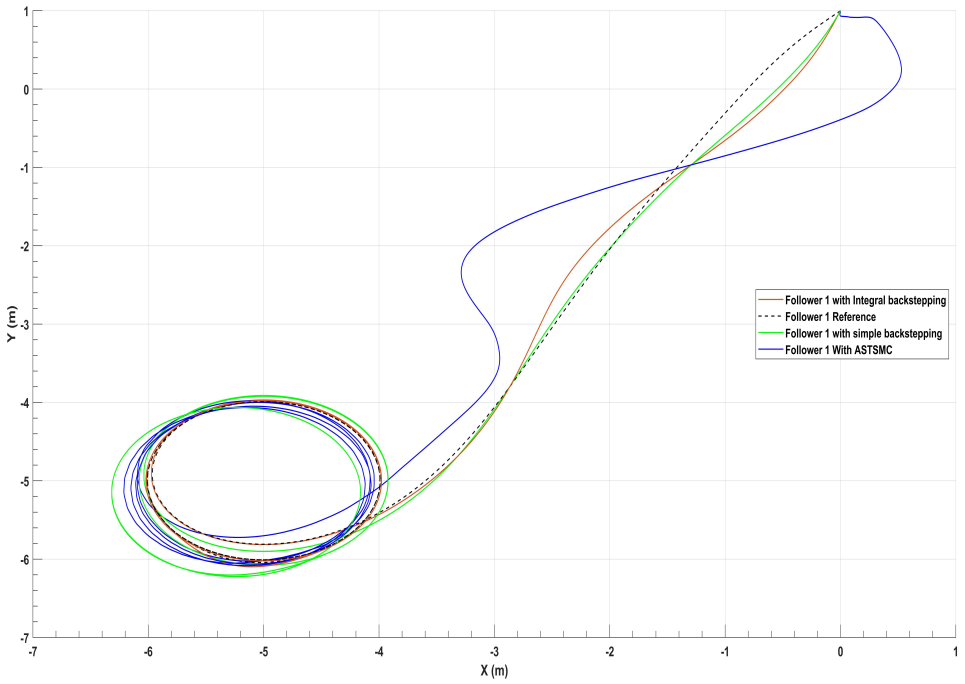

FIGURE 5.4: Trajectory tracking of Follower 1 XY under wind disturbance

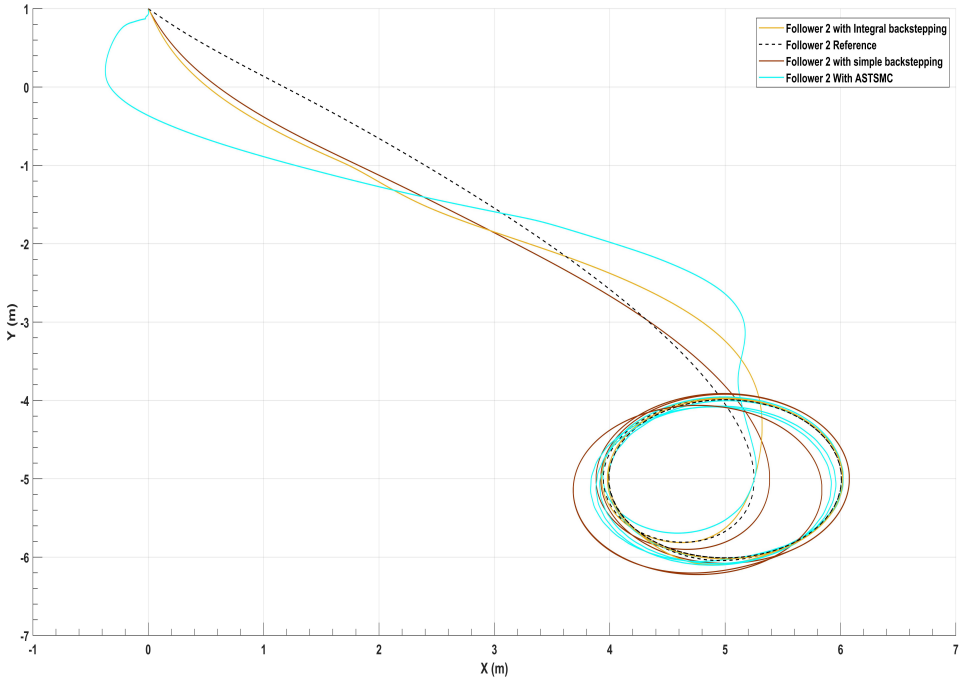

FIGURE 5.5: Trajectory tracking of Follower 2 XY under wind disturbance

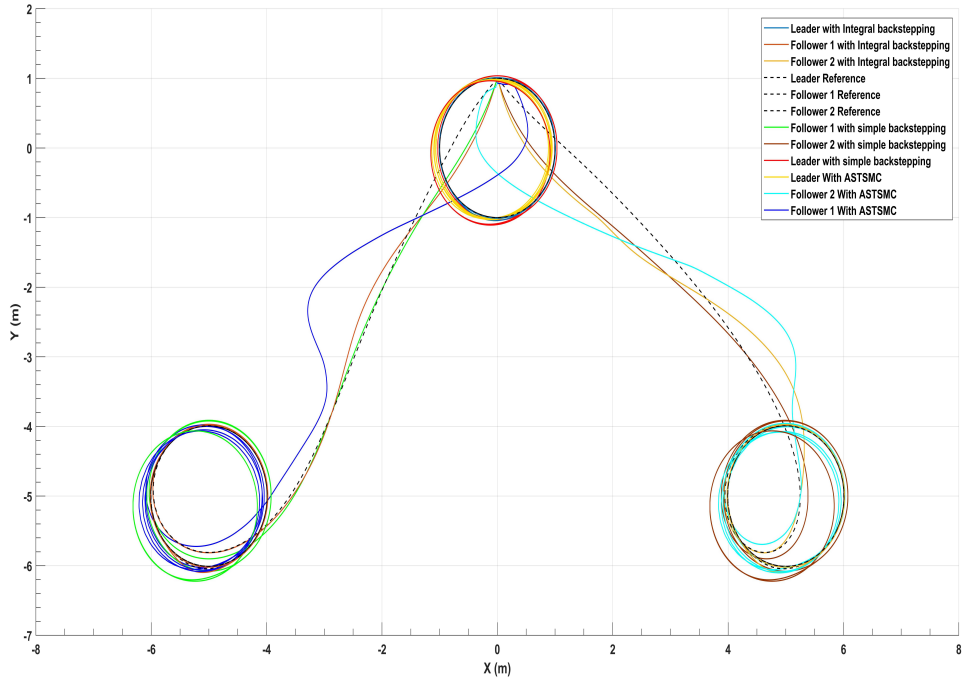

FIGURE 5.6: Trajectory tracking of Leader-Followers XY under wind disturbance

Similarly from Fig. 5.8, the e_{YL} tracking error is 0.12m with simple backstepping controller, 0.042m with ASTSMC, and 0.039m with integral backstepping controller. As integral backstepping ensures robustness and the lowest error. furthermore, suitable compensation was added by adaptive term D_{YL} of ASTSMC to neutralize the external disturbance by switching to -100. Similarly, for follower 1 and follower 2 the X and Y trajectories with respect to time, errors, and adaptive terms are represented in Fig. 5.9-5.12.

Fig. 5.13 and 5.14 shows θ and ϕ tracking performance for leader and follower UAVs with ASTSMC, simple backstepping and integral backstepping controller respectively. From the outcome and external disturbance applied at $t = 15s$, it is cease that the proposed integral backstepping controller shows better performance at tracking the desired θ and ϕ reference commands. Furthermore, Fig. 5.15 and 5.16 shows the dissimilarity between θ and ϕ in correspondence with their generated reference and commands using ASTSMC, simple backstepping, and integral backstepping controllers. From this outcome, it is apparent that this

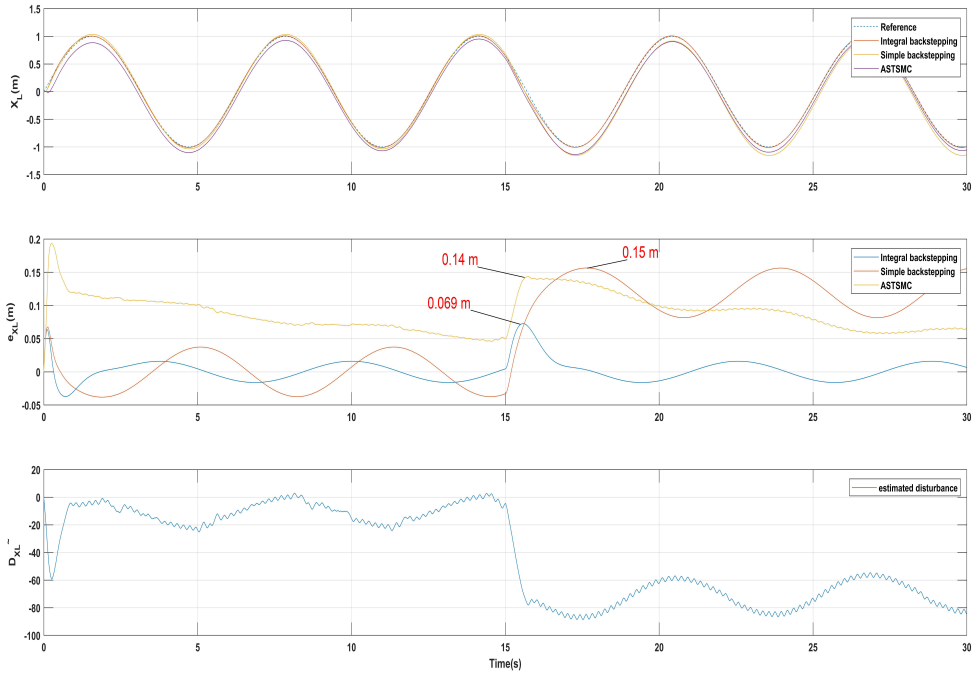

FIGURE 5.7: Trajectory tracking of X_{Leader} under wind disturbance

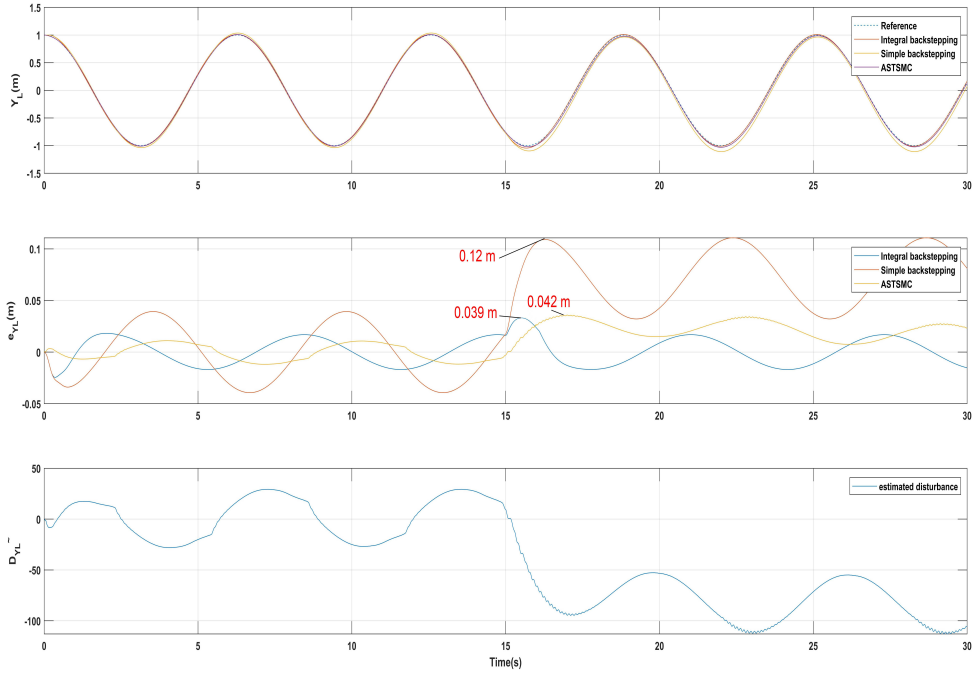

FIGURE 5.8: Trajectory tracking of Y_{Leader} under wind disturbance

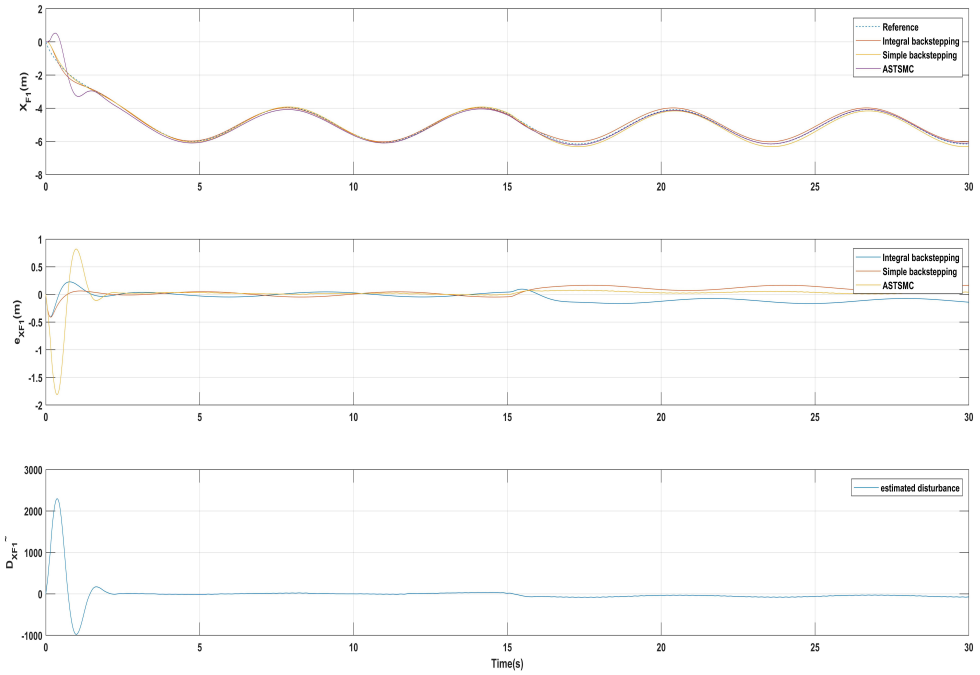

FIGURE 5.9: Trajectory tracking of $X_{Follower1}$ under wind disturbance

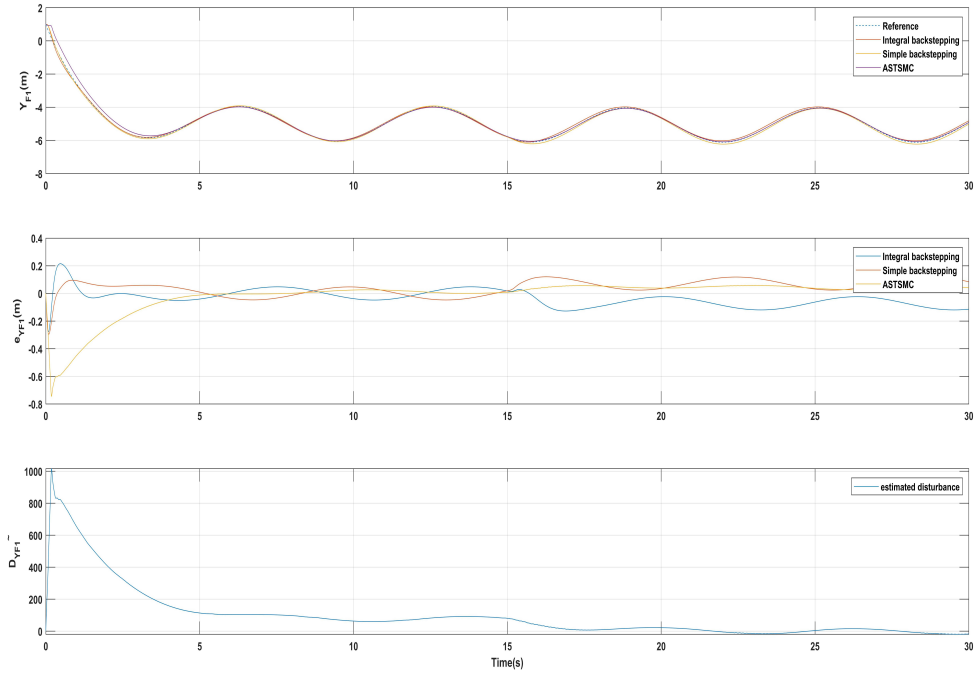

FIGURE 5.10: Trajectory tracking of $Y_{Follower1}$ under wind disturbance

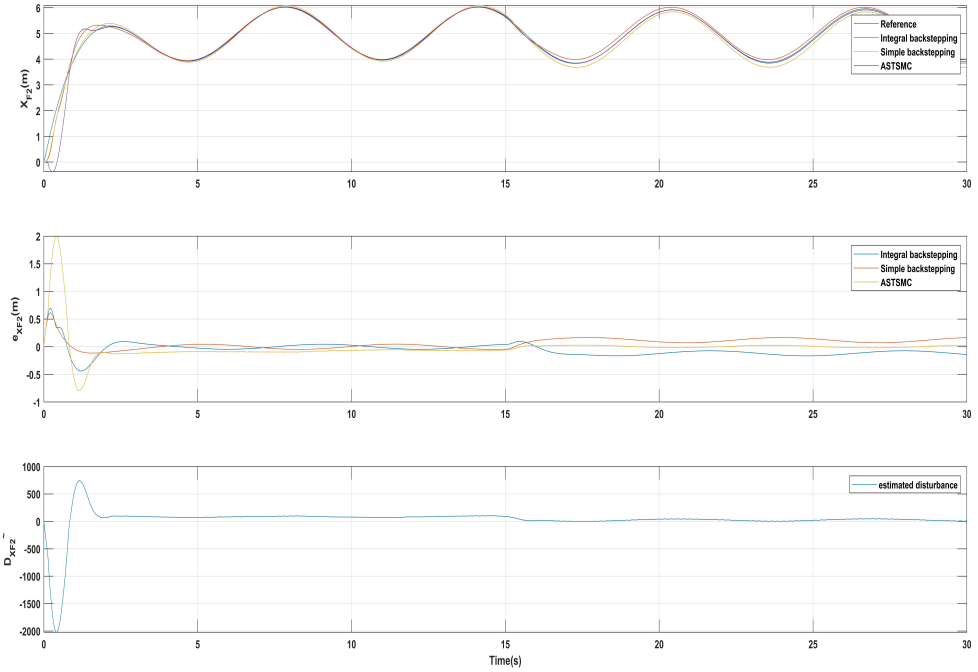

FIGURE 5.11: Trajectory tracking of $X_{Follower2}$ under wind disturbance

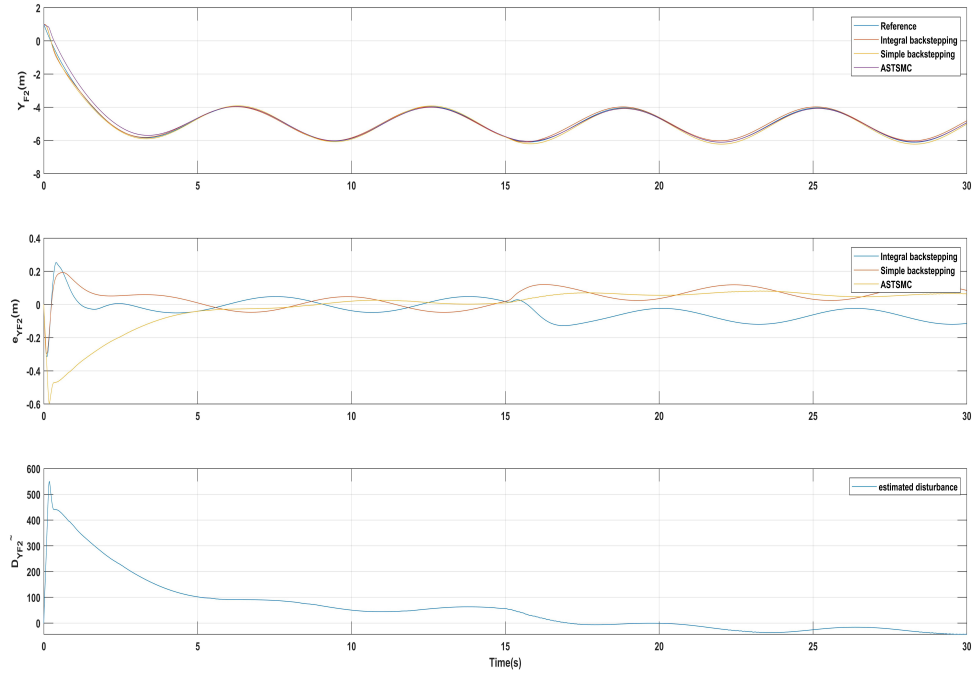

FIGURE 5.12: Trajectory tracking of $Y_{Follower2}$ under wind disturbance

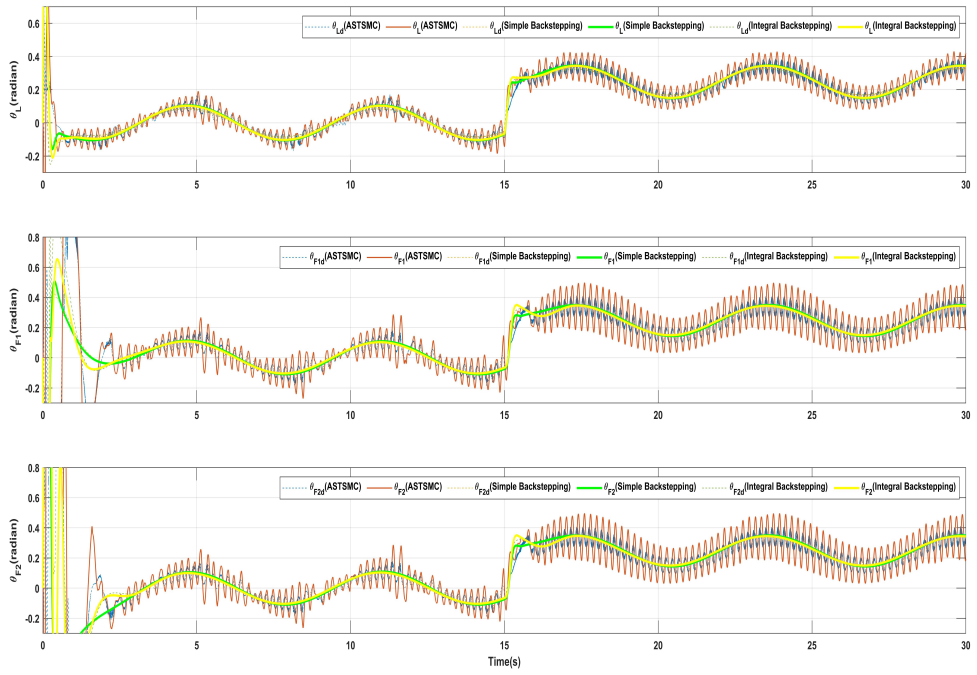

FIGURE 5.13: Tracking comparison of θ under wind disturbance

proposed integral backstepping controller produces suitable reference commands for θ and ϕ for the required leader and follower UAVs.

For leader and followers' UAVs, on ψ and Z loops since there are no external disturbances applied, their behavior with each controller is almost the same as presented in Fig. 5.17 and 5.18. Fig. 5.19 shows the formation controller robustness for tracking the reference commands in the X and Y plane of the followers' UAVs. Required distance is explicitly sustained between the followers' UAVs and their respective leader UAV from this outcome, beside the transient errors.

Finally, Fig. 5.20 represents the proposed control scheme inputs simulation results. For a clear view of the simple and integral backstepping controller, it is separately represented in Fig. 5.21. From the presented results, it is concluded that the integral backstepping controller performs greatly without any high-frequency chattering phenomena noticed at the ASTSMC controller, as chattering phenomena reduce the lifespan of the actuators, also integral backstepping controller shows great performance with trajectory tracking under wind disturbance. Moreover,

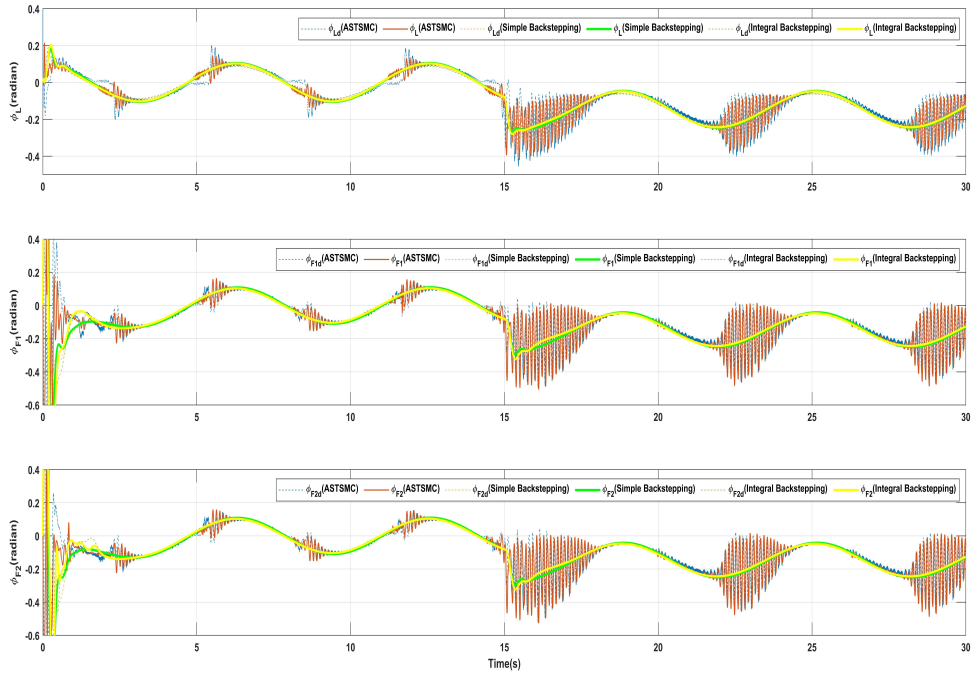

FIGURE 5.14: Tracking comparison of ϕ under wind disturbance

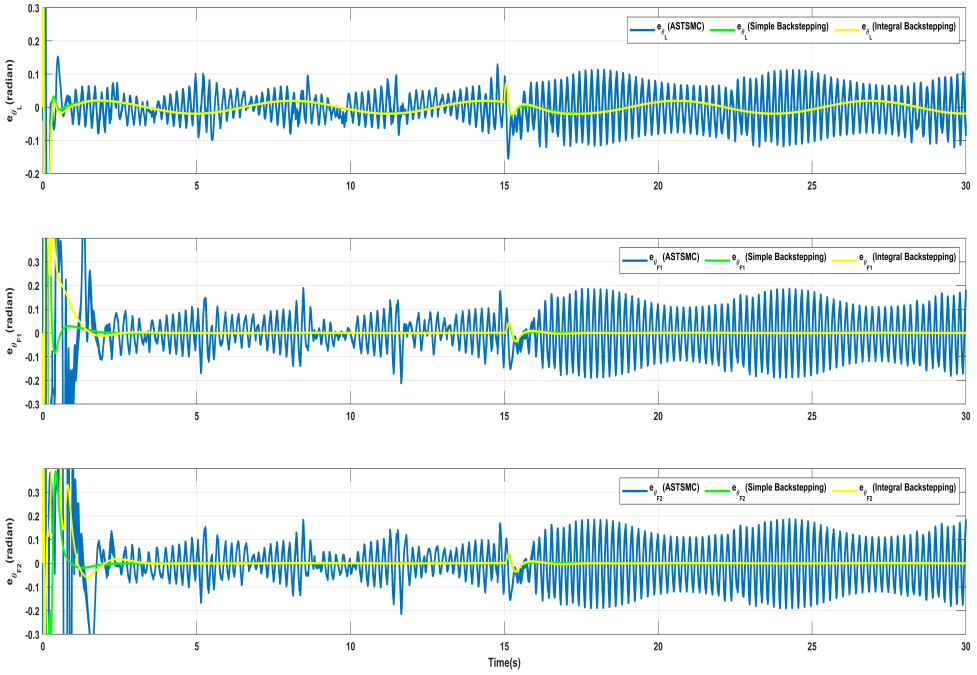

FIGURE 5.15: Difference between desired θ and commanded θ under wind disturbance

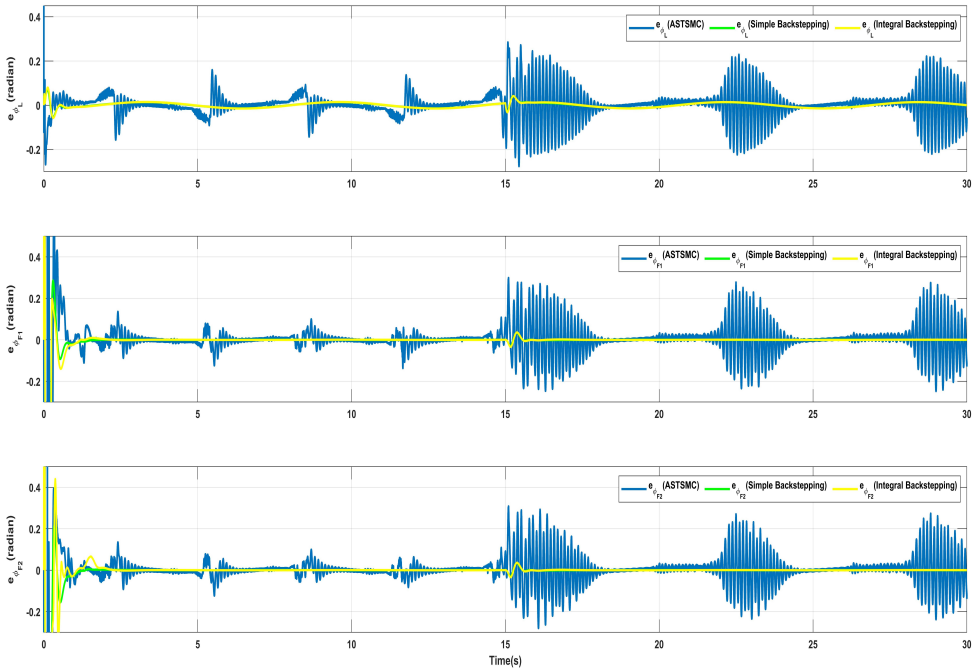

FIGURE 5.16: Difference between desired ϕ and commanded ϕ under wind disturbance

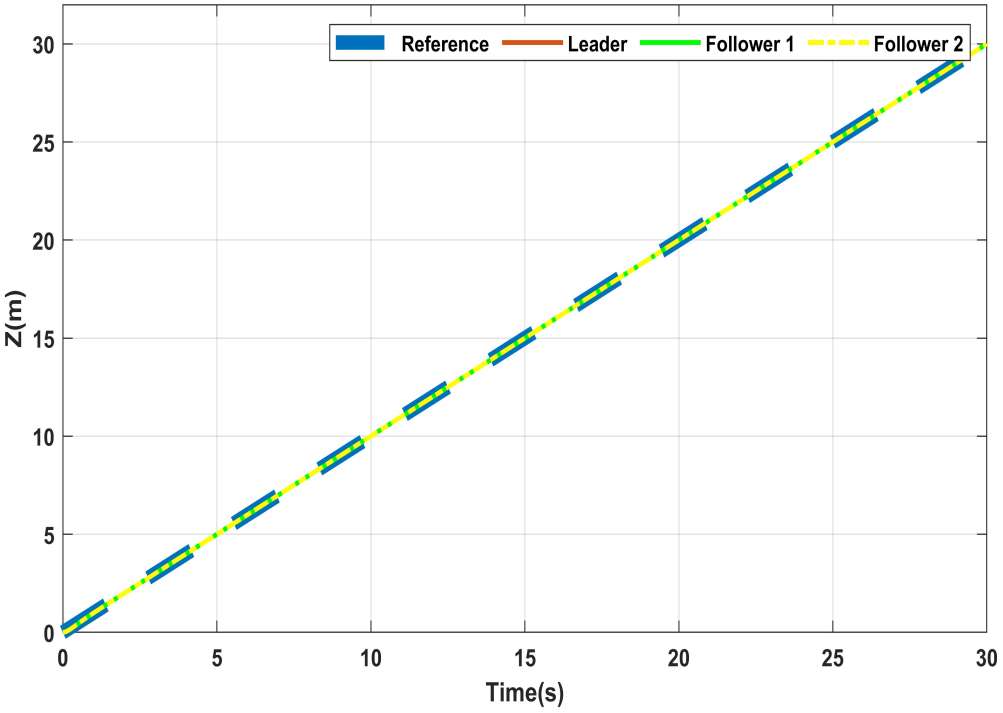

FIGURE 5.17: Difference between desired Z and commanded Z tracking

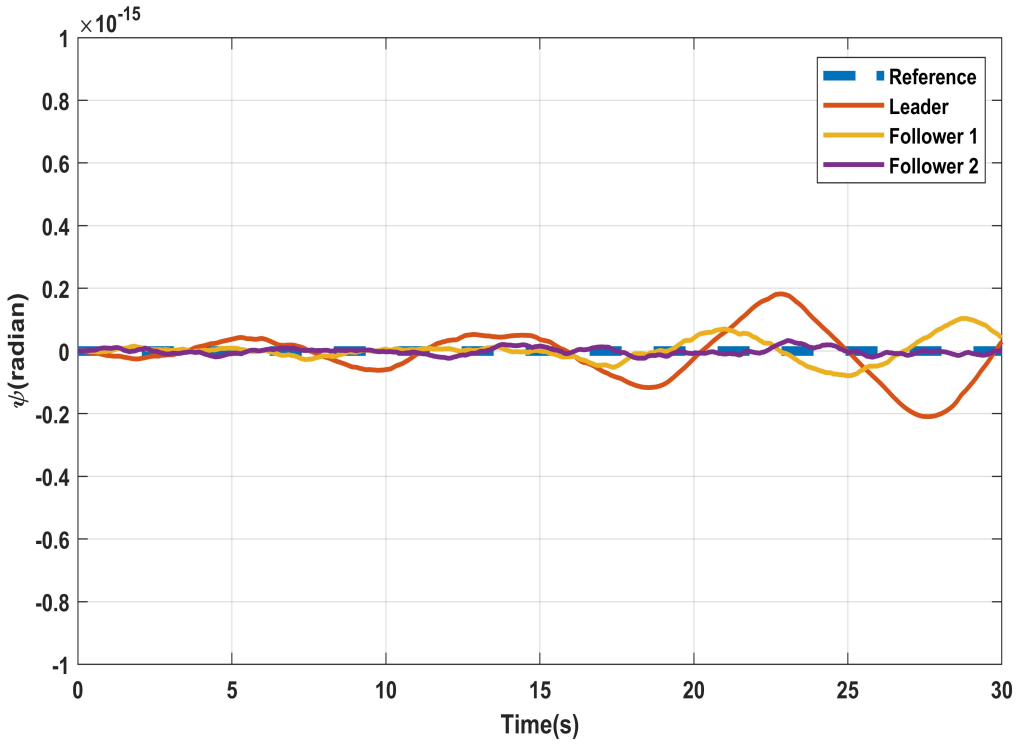

FIGURE 5.18: Difference between desired ψ and commanded ψ tracking

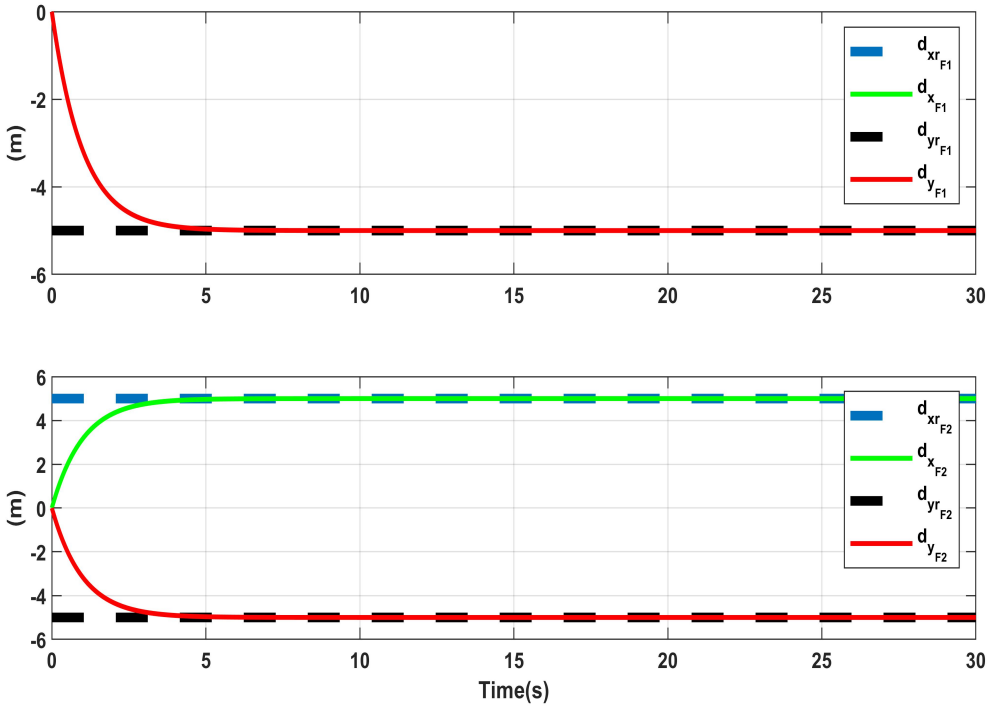

FIGURE 5.19: Formation controller tracking

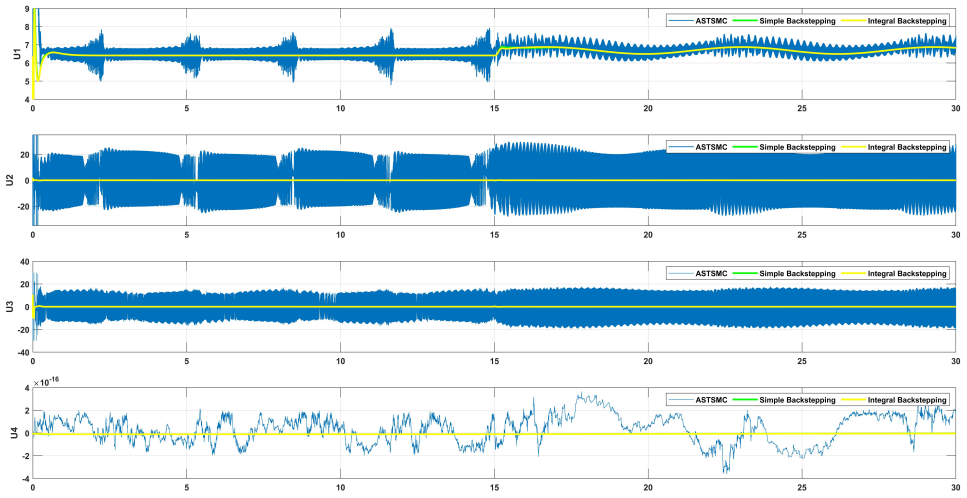

FIGURE 5.20: Control inputs of proposed control schemes

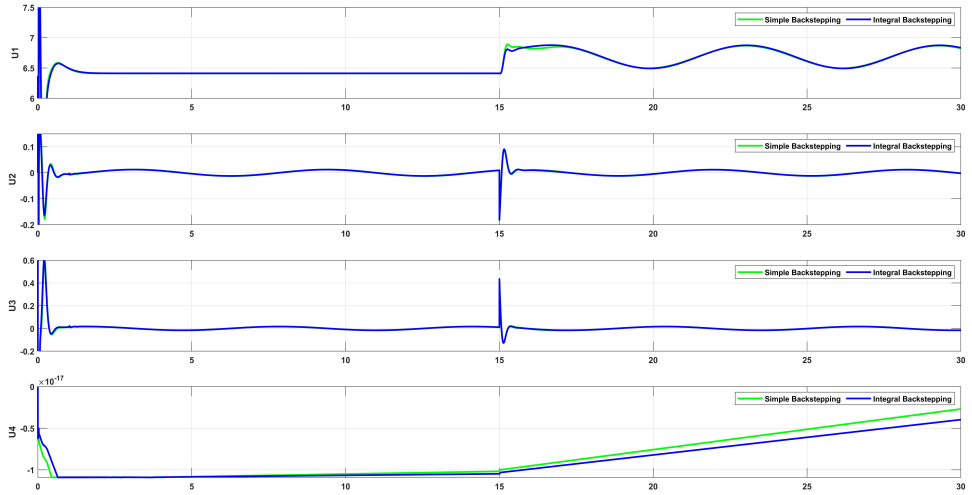

FIGURE 5.21: Control inputs of simple and integral backstepping controller

the virtual X, Y control output represented in Fig.5.13 and 5.14 of the integral backstepping controller also show no chattering phenomena and great performance with trajectory tracking under wind disturbances.

5.1 Summary

The MATLAB Simulink software has been utilised for the simulations, providing results are explained in great detail in this chapter. The proposed integral backstepping controller's robust performance is validated with the least amount of error in monitoring the intended reference trajectories in all UAV dynamics under wind disturbance. Additionally, it is demonstrated that the proposed integrated backstepping controller exhibits no chattering in control signals, in contrast to the ASTSMC, which exhibits increased chattering and shortens the life of the actuators.

Chapter 6

Conclusion and Future Work

6.1 Conclusion

This thesis presents an integral backstepping controller and a comparison with a simple backstepping controller, and ASTSMC controller for trajectory and formation controllers for leader-follower configuration. Parametric uncertainties and wind disturbance in the form of external acceleration disturbance are applied to the leader and follower UAVs X and Y dynamics.

The robust performance of the proposed controller integral backstepping controller is verified with minimum error in tracking the desired reference trajectories in all dynamics of the UAV under wind disturbance. It is also presented that the proposed controller integral backstepping controller shows no chattering phenomena in control signals while ASTSMC shows greater chattering phenomena which reduce the life of the actuators, thus controllers which show chattering phenomena are not favorably considered idle for the practical life implementation.

Moreover, the formation controllers using the proposed controller's integral backstepping controller accurately maintain the desired distance between the leader and each follower's UAV, but the ASTSMC controller exhibits starting transient error.

6.2 Future Work

Following areas could be focus for future work:

1. Implementation of proposed controllers on real quad-copter hardware.

2. The length of time it takes for sensor data to be acquired, analyzed, and then used to operate the aircraft is referred to as the sampling delay. This delay can be caused by a number of variables, including the frequency with which the sensors are polled, the time required to analyze sensor data, and communication latency between the multiple quad-copters and the ground control station. In general, the objective would be to reduce sampling latency so that the quad-copter responds to inputs as rapidly as feasible. If the sampling delay is too large, it can lead to unstable or unpredictable flight behavior.

3. Fault identification, whenever a leader UAV stops working due to any condition, one of the follower UAV take becomes the leader and other UAVs start following that leader in a specific leader-follower configuration.

4. Designing adaptive controller for mass varying UAV for multiple applications

Bibliography

[1] Shakhatreh H, Sawalmeh AH, Al-Fuqaha A, Dou Z, Almaita E, Khalil I, Othman NS, Khreishah A, Guizani M. Unmanned aerial vehicles (UAVs): A survey on civil applications and key research challenges. *IEEE Access*. 2019 Apr 9;7:48572-634.

[2] Özbek NS, Önkol M, Efe MÖ. Feedback control strategies for quadrotor-type aerial robots: a survey. Transactions of the Institute of Measurement and Control. 2016 May;38(5):529-54.

[3] Kacimi A, Mokhtari A, Kouadri B. Sliding mode control based on adaptive backstepping approch for a quadrotor unmanned aerial vehicle. Przeglad Elektrotechniczny. 2012 Jan 1;88(6):188-93.

[4] Liu X, Wang H, Fu D, Yu Q, Guo P, Lei Z, Shang Y. An area-based position and attitude estimation for unmanned aerial vehicle navigation. Science China Technological Sciences. 2015 May 1;58(5):916-26.

[5] Dinh TX, Nam DN, Ahn KK. Robust attitude control and virtual reality model for ariquadrotor. International Journal of Automation Technology. 2015 May 5;9(3):283-90.

[6] Madani T, Benallegue A. Sliding mode observer and backstepping control for a quadrotor unmanned aerial vehicles. In 2007 American Control Conference 2007 Jul 9 (pp. 5887-5892). IEEE.

[7] Alothman Y, Jasim W, Gu D. Quad-rotor lifting-transporting cable-suspended payloads control. In 2015 21st International Conference on Automation and Computing (ICAC) 2015 Sep 11 (pp. 1-6). IEEE.

[8] Dierks T, Jagannathan S. Output feedback control of a quadrotor UAV using neural networks. IEEE transactions on neural networks. 2009 Dec 4;21(1):50-66.

[9] Cruz PJ, Oishi M, Fierro R. Lift of a cable-suspended load by a quadrotor: A hybrid system approach. In 2015 American Control Conference (ACC) 2015 Jul 1 (pp. 1887-1892). IEEE.

[10] Mofid O, Mobayen S. Adaptive sliding mode control for finite-time stability of quad-rotor UAVs with parametric uncertainties. ISA transactions. 2018 Jan 1;72:1-4.

[11] Wua F, Chen J, and Liang Y. Leader–follower formation control for quadrotors. IOP Conf Series: Mater Sci Eng 2017; 187: 012016.

[12] Abbas R and Wu Q. Tracking Formation control for multiple Quadrotors based on fuzzy logic controller and least square oriented by genetic algorithm. Open Autom Contr Syst J 2015; 7: 842–850.

[13] Khaled AG and Youmin Z. Formation control of multiple quad-rotors based on leader-follower method. International conference on unmanned aircraft systems (ICUAS), Denver, CO, 2015, pp. 1037–1042.

[14] Mu B, Zhang K, and Shi Y. Integral sliding mode flight controller design for a quad-rotor and the application in a heterogeneous multi-agent system. IEEE Trans Ind Electron 2017; 64(2): 9389–9398.

[15] Mercado D A, Castro R, and Lozano R. Quad-rotors flight formation control using a leader follower approach. In: 2013 European control conference (ECC), Zurich, 2013, pp. 3858–3863.

[16] Abas MFB, Pebrianti D, Azrad S, et al. Circular leader–follower formation control of quad-rotor aerial vehicles. J Robot. 2012; 25, pp. 60-71

[17] Hua C, Chen J, and Li Y. Leader–follower finite-time formation control of multiple quad-rotors with prescribed performance. Int J Syst Sci 2017; 48(12): 2499–2508.

[18] Abdessameud A, Polushin IG, and Tayebi A. Motion coordination of thrust-propelled under-actuated vehicles with intermittent and delayed communications. Syst Control Lett 2015; 79: pp. 15–22.

[19] Li NHM and Liu HHT. Formation UAV flight control using virtual structure and motion synchronization. In: 2008 American control conference, Seattle, WA, 2008, pp. 1782–1787.

[20] Turpin M, Michael N, and Kumar V. Trajectory design and control for aggressive formation flight with quad-rotors. Autonomous Rob J 2012; 33(1–2): 143–156.

[21] Adaptive Formation Control of Quad-rotor Unmanned Aerial Vehicles with Bounded Control Thrust. Chinese Journal of Aeronautics 2017, 30, 807–817, doi:10.1016/j.cja.2017.01.007

[22] Zhao W and Go HT. Quad-copter formation flight control combining MPC and robust feedback linearization. J Frankl Inst 2014; 351(3): 1335–1355. ISSN: 0016-0032.

[23] Tiago TR, Andr´e GSC, Inkyu S, et al. Nonlinear model predictive formation control for quad-copters. IFAC-Papers OnLine 2015; 48(19): 39–44. ISSN: 2405-8963.

[24] Ariyibi, S.; Tekinalp, O. Modeling and Control of Quadrotor Formations Carrying a Slung Load. In 2018 AIAA Information Systems-AIAA Infotech @ Aerospace; American Institute of Aeronautics and Astronautics. pp. 7-8

[25] Ghommam, J.; Luque-Vega, L.F.; Saad, M. Distance-Based Formation Control for Quadrotors with Collision Avoidance via Lyapunov Barrier Functions Available [online]: https://www.hindawi.com/journals/ijae/2020/2069631

[26] Estevez J, and Grana M. Improved control of DLO transportation by a team of quadrotors. In: Ferra´ndez VJ, A´ lvarezSa´nchez J, de la Paz LF, Toledo MJ, and Adeli H. (eds) Biomedical Applications Based on Natural and Artificial

Computing. IWINAC 2017. Lecture Notes in Computer Science, vol 10338, pp. 117–126.

[27] Liang, Y.; Dong, Q.; Zhao, Y. Adaptive Leader–Follower Formation Control for Swarms of Unmanned Aerial Vehicles with Motion Constraints and Unknown Disturbances. Chinese Journal of Aeronautics 2020, 33, 2972–2988, doi:10.1016/j.cja.2020.03.020.

[28] Máthé, K.; Buşoniu, L. Vision and Control for UAVs: A Survey of General Methods and of Inexpensive Platforms for Infrastructure Inspection. Sensors 2015, 15, 14887-14916. https://doi.org/10.3390/s150714887

[29] G. Zames, "Feedback and optimal sensitivity: Model reference transformations, multiplicative seminorms, and approximate inverses,"IEEE Transactions on Automatic Control, vol. 26, no. 2, pp. 301–320, 1981.

[30] D. McFarlane and K. Glover, "A loop shaping design procedure using H infinity synthesis," IEEE Transactions on Automatic Control, vol. 31, no. 12, pp. 1799–1819, 1992.

[31] J. C. Doyle, K. Glover, , P. P. Khargonekar, and B. A. Francis, "State space solutions to standard H2 and H infinity control problem," IEEE Transactions on Automatic Control, vol. 34, no. 8, pp. 1228–1240, November 1989.

[32] P. Gahinet and P. Apkarian, "A linear matrix inequality approach to H∞ control," International Journal of Robust and Nonlinear Control, vol. 4, no. 4, pp. 421–448, 1994.

[33] Choi HS, Park YH, Cho Y, Lee M. Global sliding mode control. IEEE Control Magazine, 2001, 21(3): 27-35.

[34] Edwards C, Spurgeon S. Sliding Mode Control: Theory and Applications, London: Taylor and Francis, 1998, 1, pp.121-150.

[35] Gouaisbaut F, Dambrine M, Richard JP. Robust control of delay systems: a sliding mode control, design via LMI, Systems & Control Letters 46 (2002): 219-230.

[36] Ramirez HS, Santiago OL. Adaptive dynamical sliding mode control via backstepping, Proceedings of the 32th Conference on Decision and Control, San Antonia, Texas, December, 1992, 1422-1427.

[37] Ebrahim A, Murphy GV. Adaptive backstepping controller design of an inverted pendulum, Proceedings of the Thirty-Seventh Southeastern Symposium on System Theory, 2005, 172-174.

[38] Mehmood, Y.; Aslam, J.;Ullah, N.; Chowdhury, M.S.; Techato, K.; Alzaed, A.N. Adaptive Robust Trajectory Tracking Control of Multiple Quad-Rotor UAVs with Parametric Uncertainties and Disturbances. Sensors 2021, 21, 2401. [online]: https://doi.org/10.3390/s21072401

[39] JJE Slotine, Nonlinear applied control , W Li - Prentive Hall, Englewood Cliffs, NJ (USA), 1991, pp. 14-157

[40] [online]: https://interestingengineering.com/innovation/a-brief-history-of-drones-the-remote-controlled-unmanned-aerial-vehicles-uavs

[41] [online]: https://dronecenter.bard.edu/what-you-need-to-know-about-drone-swarms/